

**“Plant-mediated green synthesis of zinc oxide nanoparticles from  
*Alocasia odora* leaves”**

**ANNAPOORANI M  
21PCH004**

**Thesis submitted to  
Avinashilingam Institute for Home Science and Higher Education for  
Women,  
Coimbatore-641 043**

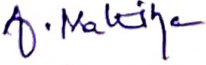
**In Partial Fulfillment of the Requirements for the Degree of  
Master of Science in Chemistry  
May - 2023**

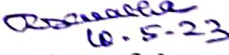
**Plant-mediated green synthesis of zinc oxide nanoparticles from  
*Alocasia odora* leaves**

**ANNAPOORANI M  
21PCH004**

**Thesis submitted to  
Avinashilingam Institute for Home Science and Higher Education for Women  
Coimbatore- 641 043**

**In Partial Fulfilment of the Requirements for the Degree of  
MASTER OF SCIENCE IN CHEMISTRY  
May – 2023**

  
Signature of the  
Supervisor

  
Signature of the  
Head of the Department

# *Acknowledgement*

## ACKNOWLEDGEMENT

First and foremost, I thank **LORD ALMIGHTY** for his blessings and giving me the strength to carry out my research work successfully.

I take enormous pleasure in thanking **Dr. S.P. THYAGARAJAN**, Chancellor Avinashilingam Institute for Home Science and Higher Education for Women, Coimbatore, for providing the favourable infrastructure to do my research work.

I would like to thank **Dr. V. BHARATHI HARISHANKAR**, Vice Chancellor, Avinashilingam Institute for Home Science and Higher Education for Women, Coimbatore, for the encouragement and for providing the opportunity to develop and establish my skills.

I extend my thanks to **Dr. S. KOWSALYA**, Registrar, Avinashilingam Institute for Home Science and Higher Education for Women, Coimbatore, for the encouragement given by her during the investigation.

I express my heartfelt thanks to **Dr. G. PADMAVATHI**, Professor, Dean, School of Physical and Computational Sciences, Avinashilingam Institute for Home Science and Higher Education for Women, Coimbatore, for her excellent support, unflinching encouragement and guidance during the course of the investigation.

I record my deep sense of gratitude to **Dr. (Mrs) R. SARATHA, Professor and Head of the Department**, Department of Chemistry, Avinashilingam Institute for Home Science and Higher Education for Women, Coimbatore, for her constant support and tremendous care rendered for carrying out of my thesis successfully.

I extend my deep sense of gratitude to my guide **Dr. (Mrs.) A. MATHINA Assistant Professor** , Avinashilingam Institute for Home Science and Higher Education for Women, University Coimbatore for her guidance, encouragement and excellent support for the successful completion of the study.

I extend my deep sense of gratitude to my guide **Dr. (Mrs.) A. PRITHIBA Assistant Professor**, Avinashilingam Institute for Home Science and Higher Education for Women, University Coimbatore for her guidance, encouragement and excellent support for the successful completion of the study.

I would like to express my sincere thanks to all the **STAFF MEMBERS OF THE DEPARTMENT OF CHEMISTRY**, Avinashilingam Institute for Home Science and Higher Education for Women, University Coimbatore, for their help and support in the successful completion of this dissertation.

My special thanks to my seniors **S.THARANI, C.DHIVYA** for their presents ,advice and support whenever needed during my studies.

My special thanks to my **BELOVED PARENTS** and **SISTER** for their help whenever required to complete this work.

I also thank **ALL MY FRIENDS** for their continuous encouragement and support throughout the work.

**ANNAPOORANI M**

# *Contents*

## CONTENT

<b>S.No</b>	<b>List</b>	<b>Page No</b>
	List of Figures	XIX
	List of Tables	VI
	List of Abbreviations	VI
1	Introduction	1
2	Review of literature	12
3	Materials &Methods	32
4	Results Discussion	42
5	Summary and Conclusion	58
6	Bibliography	60

## LIST OF FIGURES

<b>S.No.</b>	<b>Figure No.</b>	<b>Title</b>	<b>Pag No.</b>
1	1.1	Structure of zinc oxide nanoparticles	2
2	1.2	Properties of zinc oxide nanoparticles	4
3	1.3	Terahedral structure of ZnO NPs	5
4	1.4	Application of ZnO NPs	7
5	1.5	Image of alocasia odora leaf	8
6	4.1.1	Preliminary phytochemical screening	43
7	4.2.1	UV-Spectrum of ZnO NPs	44
8	4.2.2	Tauc plot of ZnO NPS	45
9	4.2.3	FT-IR image of ZnO NPs	46
10	4.2.4	SEM image of ZnO NPs	48
11	4.2.5	EDAX image ZnO NPs	48
12	4.2.6	3D optcal profilometer image of ZnO NPs	50
13	4.2.7	Histogram image of ZnO NPs	50
14	4.2.8	Cross image of ZnO NPs	51
15	4.2.9	Roughness image of ZnO NPs	51
16	4.2.10	TG image of ZnO NPs	52
17	4.2.11	TG DTG image of ZnO NPs	53
18	4.2.12	Inhibition zone of ZnO NPs	54
19	4.8.13	XRD image of ZnO NPs	55

## LIST OF TABLES

<b>S.NO</b>	<b>TABLE.NO</b>	<b>TITLE</b>	<b>PAGE.NO</b>
1	1.1	Scientific classification of alocasia odora leaf	8
2	4.1.1	Phytochemical constituents alocasia odora leaf extract	47
3	4.2.1	FT-IR spectr range and functional group of ZnO NPs	49
4	4.2.2	EDX value of ZnO NPs	44
5	4.2.3	Zone of inhibition	55
6	4.2.4	Structure and geometric	56

## LIST OF ABBREVIATIONS

UV	Ultra Violet Spectroscopy
FT-IR	Fourier Transform Infrared Spectroscopy
SEM	Scanning electron microscopy
EDAX	Energy dispersive X-ray analysis
TGA	Thermo gravimetric analysis
XRD	X-Ray Diffraction

# *Introduction*

## 1. INTRODUCTION

Zinc oxide nanoparticles are nanoparticles of zinc oxide (ZnO) that have diameters less than 10 nanometers. They have a large surface area relative to their size and high catalytic activity. The exact physical and chemical properties of zinc oxide nanoparticles depend on the different ways they are synthesized. Some possible ways to produce ZnO nano-particles are laser ablation, hydrothermal methods, electrochemical depositions, sol–gel method, chemical vapor deposition, thermal decomposition, combustion methods, ultrasound, microwave-assisted combustion method, two-step mechanochemical–thermal synthesis, anodization, co-precipitation, electrophoretic deposition, and precipitation processes using solution concentration, pH, and washing medium. ZnO is a wide-band gap semiconductor with an energy gap of 3.37 eV at room temperature. Recent years have seen a surge in interest in ZnO semiconductors due to their novel and alluring applications in a range of industries, including chemistry, physics, biology, film, electronics, and more. They may possess these characteristics as a result of their high surface area, compact size, and availability of surface-specific binding sites, catalytic, electronic, and medicinal activities. ZnO-NPs, which are commonly used as dispersions or powders in a variety of items like calamine lotion, baby powder, ceramics, UV filters, ointments, paints, food additives, and other things, are readily available for purchase. **Chanu *et.al.*,(2019)**



**Figure: 1.1 Structure of zinc oxide nanoparticles**

The unique features of nanoparticles (NPs), which originate from their sub 100 nm dimensions, are being used by a range of industries to give many products improved function. Consumers now commonly come across NPs in everyday products including paint, clothing, cosmetics, and textiles. Higher creation of NPs is also being fueled by new construction materials, catalysts, electronics, and optical devices. The medical industry is creating NPs for real-time sensing, tumor-specific hyperthermia therapy, analytical tests, and medication delivery.

Due to its distinctive and alluring features, zinc oxide nanoparticles (ZnO NPs) have attracted a great deal of attention from scientists. Because of its unique antibacterial, antifungal, wound-healing, and UV filtering characteristics, as well as its strong catalytic and photochemical action, ZnO NPs have recently gained attention from the scientific community. It's interesting that scientists have immobilised beta galactosidase using ZnO nanoparticles.

The modified version of basic elements, known as NPs, are tiny molecule aggregates less than 100 nm in size that have unusual properties in comparison to their bulk constituents. They have significant adsorption capacity, high surface energy, high surface to volume ratio, and high catalytic efficiency. These exceptional qualities of NPs have drawn numerous researchers in recent years to offer fresh answers in a variety of scientific domains. The special qualities of NPs have made it possible to achieve sustainable agriculture and safeguard the future. NPs have the potential to be a tool for increasing plant output and growth. NPs could mitigate the negative effects on the environment and non target plant tissue.

To boost plant growth, they can be utilized as herbicides, nanopesticides, and nanofertilizers. The toxicity that NPs convey to plants and the environment, however, cannot be ignored. The form, size, chemical composition, surface energy, solubility, and species of NPs affect their toxicity to plants. To use NPs wisely and increase crop output, a greater understanding of their function in plants is required.

The exceptional physical, optical, and antibacterial properties of zinc oxide nanoparticle (ZnO NP), a metal based NP, make it an essential NP among the different types of NPs. ZnO NP also has a wide range of applications. Zinc does not interact with the majority of pharmaceutically active compounds, making ZnO NPs less poisonous, comparably inexpensive, and biocompatible than other metal oxide NPs. The Food and Drug Administration has designated ZnO as a substance that is "generally regarded as safe" (GRAS) and is used as a food additive. ZnO NPs play a critical role in the growth and development of plants, according to numerous studies; larger concentrations, however, have detrimental effects on plants.

## Properties of ZnO NPs

Inorganic chemical zinc oxide is a white powder that is almost completely insoluble in water. The crust of the earth contains it as the mineral zincite. Zinc oxide is also referred to as a group II-VI semiconductor since zinc and oxygen are members of groups II and VI, respectively, of the periodic table. Due to its exceptional qualities, ZnO NPs have been used in a variety of fields. One-dimensional, two-dimensional, and three-dimensional structures are all possible for zinc oxide.

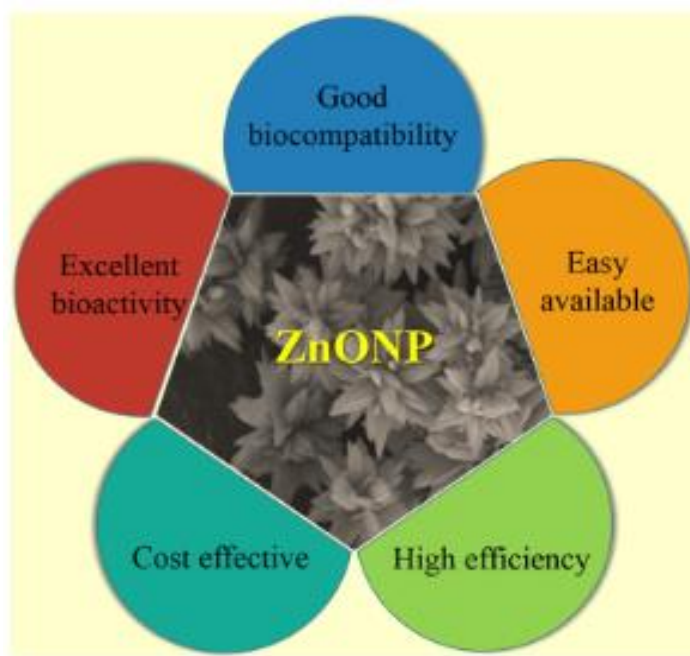


**Figure: 1.2 Properties of zinc oxide nanoparticles**

The majority of the structures seen in one-dimensional ZnO are nanorods, needles, helices, springs, rings, ribbons, tubes, belts, wires, and combs. Nanoplates/nanosheets and nanoparticles are examples of two-dimensional structures, while flowers, dandelions, snowflakes, and formations resembling sea urchins are examples of three-dimensional structures; Bitenc and Oreš. ZnO NPs are useful in optoelectronics and electronics because of their 3.37 eV broad energy band, 60 meV bond energy, good thermal stability, and mechanical stability at ambient temperature.

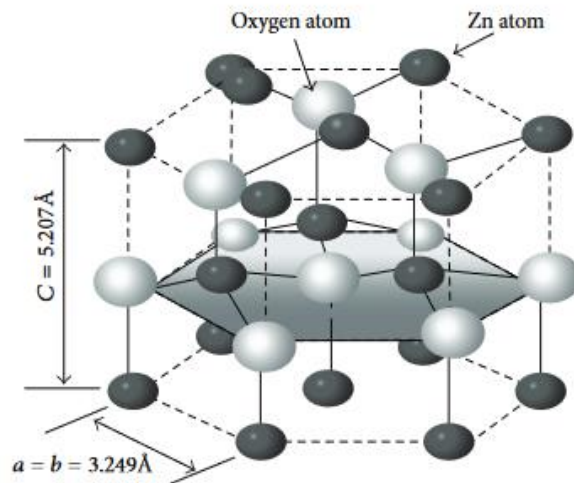


**Figure: 1. 3 Tetrahedral structure of ZnO-NPs**

In addition, ZnO nanoparticles can be employed as sensors, converters, energy producers, and photocatalysts in the hydrogen synthesis process thanks to their piezo- and pyroelectric capabilities. Included in two-dimensional structures are ZnO NPs have potential use in the biomedical field and the ceramics sector due to their hardness, firmness, targeting capability, low toxicity, biocompatibility, and biodegradability.

ZnO NPs have a larger surface area to volume ratio, which boosts their biological activity and reactivity, making them an efficient antibacterial agent. Bacterial growth has been reported to be significantly suppressed by ZnO NPs by interacting with the cell surface, changing the permeability of the cell membrane, and finally producing oxidative stress, resulting in gradual cell damage and death. Moreover, it has been demonstrated that ZnO NPs were hazardous to pathogenic bacteria but beneficial to helpful germs like *Pseudomonas putida*.

### **Application of ZnO nanoparticles**

Due to their unique features, applications of nanoparticles between 1 and 100 nm in size have drawn a lot of attention recently and are the subject of in-depth study. Characteristics of nanoparticles are distinct from those of bulk materials. Studies on the synthesis, characterisation, and characteristics of nanoparticles have drawn a lot of attention in recent years due to their various uses. ZnO nanoparticles (n-ZnO) have drawn more attention than other types of nanoparticles.

Wide band gap semiconductor ZnO has great transparency and excellent electrical conductivity in addition to having a significant excitation binding energy of 60 meV at ambient temperature. ZnO is beneficial in a variety of space applications due to its radiation damage resistance.

ZnO nanoparticles are used in a wide variety of industrial products, including biosensors, gas sensors, solar cells, ceramics, nano generators, photo detectors, catalysts, active fillers for rubber and plastic, UV absorbers in cosmetics, anti-virus agents in coatings, pigments, optical materials, cosmetics, photocatalytic, electrical and optoelectronic processes and systems, additives, and water and waste water treatment. ZnO nanoparticles have been created using a variety of methods (n-ZnO). Some of the processes used for the production of nanoparticles include sol-gel methods, spray pyrolysis, microemulsion techniques, thermal evaporation, laser ablation, chemical vapour deposition, mechanical milling, microwave approach, and hydrothermal synthesis.

Due to their high surface energy, nanoparticles do, however, tend to aggregate in the majority of these procedures. The simplest of the aforementioned methods is the solution-based approach. Using this method, the shape of the nanoparticles may be adjusted by adjusting the pH, precursor concentration, temperature, and reaction time. Due to their unusual features, nanoparticle applications have gained prominence recently and are now the subject of in-depth study. Many processes have been used to create nanoparticles, including hydrothermal synthesis, spray pyrolysis, micro-emulsion techniques, thermal evaporation, laser ablation, chemical vapour deposition, mechanical milling, photo thermal synthesis, thermal plasma synthesis, and flame synthesis.

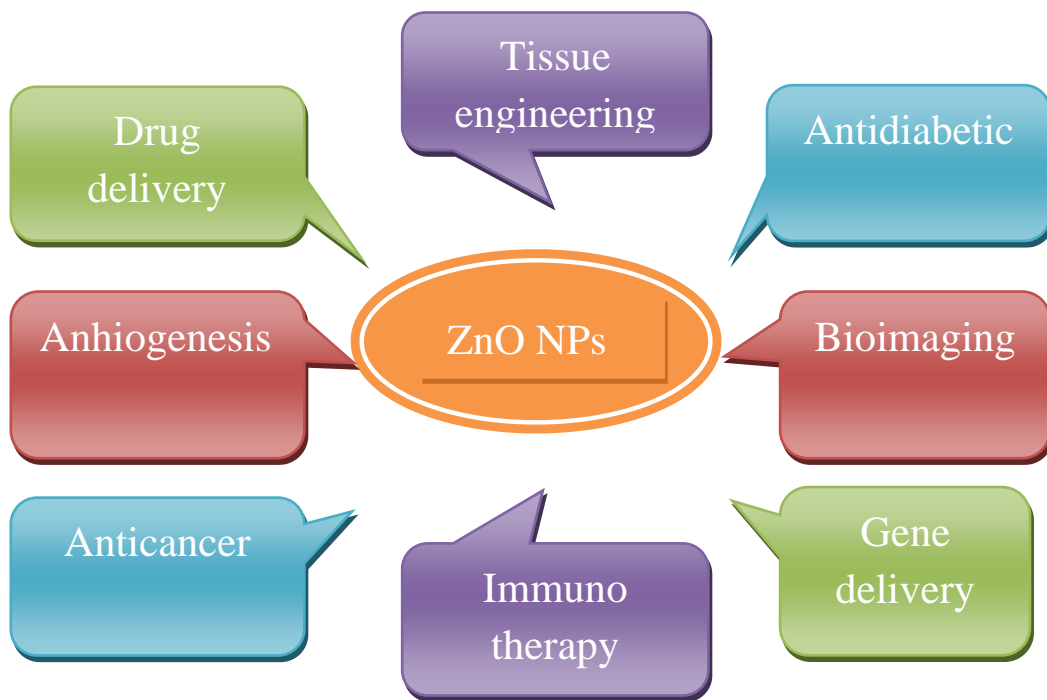


**Figure: 1.4 Application of zinc oxide nanoparticles**

The simplest and least expensive of the strategies mentioned above is the solution-based approach. The sol gel approach is used to create ZnO nanoparticles in the current study as well. Nanoparticles are distinct from bulk material particles. In

recent times, nanoparticles have been used to remediate wastewater and water. The nanoparticles have several benefits over conventional adsorbents, including a "high surface area to volume ratio."The interaction of contaminant species can occur at larger active sites in nanoparticles. In the current study, solution-based ZnO nanoparticle synthesis and several methodologies for characterising them have been carried out.



**Figure: 1.5** image of *Alocasia odora* leaf

**Scientific classification of *Alocasia odora*:**

Botanical Name	<i>Alocasia odora</i>
Kingdom	Plantae
Clade	Tracheophytes
Clade	Angiosperms
Order	Alismatales
Family	Araceae
Genus	<i>Alocasia</i>
Species	<i>A.odora</i>

**Table: 1.1** Scientific classification of *Alocasia odora*

*Alocasia odora* (also called night-scented lily, Asian taro or giant upright elephant ear) is a flowering plant native to East and Southeast Asia (Japan, China, Indochina, Assam, Bangladesh, Borneo, Taiwan). In Manipur, local name is Hoomu. *Alocasia odora* (called Ray) can be used as medicine for the treatment of common cold in North Vietnam. The plant is actually inedible when raw because of needle-shaped raphides (calcium oxalate crystals) in the plant cells.

In Japan, there are several cases of food poisoning by accidental consumption. The Ministry of Health, Labour and Welfare warned not to eat *Alocasia odora* (Kuwazuimo), which looks similar to edible *Colocasia gigantea* (Hasuimo) or *Colocasia esculenta* (Satoimo). This plant grows to about 0.5–1.6 m high, with rhizomes of about 4-10 cm high and 3-5 cm wide. The leaves are big and blade-shaped, ovate, light green with cordate base. The petioles are 0.3-1.0 m long, with the lower parts clasped around the stem

## **OBJECTIVES**

1. To synthesize ZnO nanoparticles through biosynthesis.
2. To use fewer chemicals and create less waste.
3. To characterize the synthesized ZnO nanoparticles using UV-Visible spectroscopy. FT-IR, SEM, EDAX, TGA, 3-D profilometer and perform antibacterial studies.

# *Review of Literature*

## 2. REVIEW OF LITERATURE

**Parthasarathy *et.al.*, (2016)** In this study the goal was to learn how zinc oxide nanoparticles were created and analysed using leaf extract from *Anisochilus carnosus*. The research found that the plant extract has a substantial amount of phytochemicals. The leaf extract was used to create the nanoparticles, which were then examined using UV, FTIR, SEM, and XRD. The discovery of various functional groups suggests that the extract contains a variety of chemicals. Additionally, the zinc oxide nanoparticles have strong antibacterial properties against a variety of harmful pathogens.

**Dharma Rao *et.al.*,(2016)**They synthesis of several biologically important 1,8-dioxo-octahydroxanthene derivatives, zinc oxide nanoparticles (ZnO-NPs) were used as a safe, reusable heterogeneous catalyst. This has been accomplished by employing ZnO-NPs as an environmentally friendly heterogeneous catalyst to condense different aldehydes with 5,5- Dimethyl-1,3-cyclohexanedione.Under conditions of no solvent present, the ZnO-NPs catalyst demonstrated remarkable catalytic activity to achieve the synthetic targets in the range of 80-93% yield. With a similar catalytic response, ZnO-NPs could be used for up to four cycles. Greater selectivity, cost-effectiveness, clear reaction profiles, an easy work-up process, and excellent yields were all offered by the technique.

**Parthasarathy *et.al.*,(2016)** Because they are more environmentally friendly, plants have been used in the synthesis of metallic nanoparticles. A regulated synthesis is also possible with these plant extracts. Extreme conditions are necessary for the creation of nanoparticles using harmful organic chemical solvents. Plant extracts serve as hydrolytic, capping, or stabilising agents. The ZnO nanoparticles are of great interest since they have a wide range of real-world uses. The use of ZnO nanoparticles as antibacterial agents would be their most significant use. These particles are the best antibacterial agent due to their increased surface area and smaller size. The overview of green ZnO nanoparticle production and their antibacterial activities are covered in this review. Additionally, the activity's mechanism was examined.

**Elumalai *et.al.*,(2015)** The creation of metal and semiconductor nanoparticles is a growing field of study because of the potential for use in the creation of cutting-edge technologies. Particularly, the field of nanotechnology has seen a rise in the importance of biologically produced nanomaterial.

The current study discussed the antibacterial properties of *Azadirachta indica* (L.) leaf aqueous extract used in the manufacture of zinc oxide nanoparticles (ZnO NPs). The nanoparticles were obtained and studied using a variety of techniques, including ultraviolet-visible spectroscopy, photoluminescence, X-ray diffraction, Fourier transform infrared spectroscopy, scanning electron microscopy, energy dispersive X-ray analysis, field emission scanning electron microscopy, and atomic force microscopy.

**Yuvakkumar *et.al.*, (2014)** as a natural ligation agent, *Nephelium lappaceum* L. peels was successfully employed in the manufacture of zinc oxide nanoparticles. Utilising HPLC and GC-MS studies, the contribution of rambutan extract to the synthesis of zinc oxide nanoparticles was confirmed. The crystallinity and spherical morphology of the biosynthesized nanoparticles were demonstrated by the XRD and TEM. The XRD and TEM analyses revealed that the particles had a size of 20 nm.

**Hasna Abdul Salam *et.al.*,(2014)** Researchers are becoming increasingly interested in green nanotechnology, which uses plants to create nanoparticles instead of hazardous chemicals, as an environmentally benign alternative to traditional physical and chemical approaches. In the current study, zinc nitrate and *Ocimum basilicum* L. var. *purpurascens* Benth.-LAMIACEAE leaf extract were used to create zinc oxide nanoparticles (ZnO-NPs). Using XRD, TEM, and EDX analyses, hexagonal (wurtzite) shaped ZnO-NPs with a size of about 50 nm were synthesised.

**Awwad *et.al.*,(2014)** In this study, a green approach for producing zinc oxide nanosheets and characterising them using *Olea europea* leaf extract is reported. Scanning electron microscopy (SEM), Fourier transform infrared spectroscopy

(FT-IR), X-ray diffraction (XRD), and UV-vis absorption spectroscopy were used to characterise ZnO nanosheets. ZnO nanosheets have an absorption band at 374 nm in the UV-vis absorption spectrum. The final product is described by XRD as highly crystalline ZnO with diameters between 18 and 30 nm. The SEM findings show the presence of a network of 500 nm-sized, randomly oriented ZnO nanosheets or nanoplatelets with a 20 nm average thickness. This quick and environmentally friendly method could be a helpful tool for the industrial synthesis of additional nanoparticles with biotechnological applications.

**Abdulaziz Bagabas *et.al.*,(2013)** discovered that zinc oxide nanoparticles were easily produced at room temperature using zinc nitrate hexahydrate and cyclohexylamine in either an aqueous or an ethanolic media. The calcined ZnO E had a regular polyhedra morphology, whereas the calcined ZnO W had an uneven spherical morphology with some chunky particles.

The better photocatalytic performance of ZnO E over ZnO W was attributed to its shape. The physicochemical characteristics of the synthesis medium have a considerable influence on changes in morphology and photocatalytic performance

**Sagar Raut *et.al.*, (2013)** they covered the green synthesis method's application to the production and characterisation of ZnO nanoparticles in this study. Here, we made ZnO nanoparticles by using the leaves of the *Ocimum Tenuiflorum* plant as a reducing agent. As opposed to conventional methods like the sol-gel technique, laser ablation, solvothermal, inert gas condensation, chemical reduction, etc., the green synthesis approach eliminates inert gases, high pressure, laser radiation, high temperature, hazardous chemicals, etc. By using the X-Ray diffraction (XRD), scanning electron microscopy (SEM), and Fourier Transform Infrared Spectroscopy (FTIR) techniques, prepared ZnO nanoparticles were characterised. Using Scherrer's formula, the average particle is determined to be 13.86 nm.

**Bao Ji *et.al.*, (2012)** demonstrated that the oxide nanoparticles were generated using microwave breakdown of a zinc acetate precursor. Horseradish peroxidase (HRP) was immobilised on nano-ZnO. The catalytic activity, physical and chemical

properties of immobilised HRP, as well as the interaction between HRP and nano-ZnO, were investigated. The Nano-ZnO immobilized HRP demonstrated superior thermostability and active pH stability. In the elimination of numerous phenolic chemicals, Nano-ZnO outperforms free HRP. The results suggest that nano-ZnO is a strong functional material for environmental protection.

**Abdelhady *et.al.*,(2012)** Synthesised ZnO nanoparticles were synthesised using various amounts of ZnO at various temperatures. ZnO nanoparticles in rod shape were created, with an average length of 60 nm and a width of 5–15 nm. As a result, the produced ZnO nanoparticles were analysed using a UV spectrophotometer, FTIR, TEM, X-ray, and SEM. The size and shape of ZnO nanoparticles were determined by the conditions under which they were created. Notably, ZnO rods with average lengths of 60 nm and average widths of 5–15 nm were produced. The addition of ZnO nanoparticles to cotton improved the fabric's antibacterial and UV protection characteristics. SEM, ultraviolet protection factor (UPF) rating, and antibacterial (gram-positive and gram-negative) properties were used to evaluate cotton fabric. The finished cotton fabric was antibacterial against both gram-positive and gram-negative microorganisms.

**Sheetal Chawla *et.al.* (2012)** Vanadium-doped zinc oxide nanoparticles have been made by employing the sol-gel method and supercritical drying in ethyl alcohol at 250°C. After being heated at 500 °C for two hours in a natural environment, the resulting nanopowder was analysed using a number of techniques, including particle size analysis, scanning electron microscopy (SEM), transmission electron microscopy (TEM), X-ray diffraction (XRD), and photoluminescence (PL). The powder, as prepared, has an average particle size of 25 nm and exhibits a substantial luminescence band in the visible region. Platinum (Pt) is used as the auxiliary electrode and Ag/AgCl as the reference electrode. Before the biosensor could measure the HbA1c level in the entire blood samples, the blood was hemolyzed and digested by protease. The photoluminescence excitation (PLE) band's energy location relies on the excitation wavelength, and this PL can be created by a few visible excitations.

**Paula Judith Perez Espitia *et.al.*, (2012)** The Food and Drug Administration now lists ZnO as a material that is generally regarded as safe (GRAS) and is used as a food additive. With the development of nanotechnology, novel materials with antibacterial properties have been developed. Thus, antibacterial characteristics and prospective uses in food preservation have been demonstrated by ZnO at the nanoscale. ZnO nanoparticles were embedded in polymeric matrices to enhance antimicrobial action and improve packaging qualities (38).

**Gunalan Sangeetha *et.al.*, (2011)** proposed a study of the microorganisms, enzymes, plants, or plant extracts as potential eco-friendly substitutes for chemical and physical processes in the creation of nanoparticles. In this article, they describe the chemical and biological processes used to create nanostructured zinc oxide particles. Using zinc nitrate and Aloe vera leaf extract, very stable and spherical zinc oxide nanoparticles are created. Aloe leaf broth concentrations greater than 25% have led to a conversion rate of nanoparticles of greater than 95%. UV-Vis spectrophotometer, FTIR, Photoluminescence, SEM, TEM, and XRD analyses have all been used to characterize the structural, morphological, and optical characteristics of the produced nanoparticles. The produced zinc oxide nanoparticles were polydispersed and, according to SEM and TEM examination, their average size ranged from 25 to 40.

**Varadhan Krishnakumar *et.al.*, (2011)** The synthesis of N-arylhomophthalimides and benzannelated isoquinolinones was accomplished using a straightforward, environmentally friendly methodology that the author established using a productive, heterogeneous, and recyclable catalyst called zinc oxide nanoparticles (ZnO NPs). FTIR, <sup>1</sup>H NMR, <sup>13</sup>C NMR, and HRMS techniques were used to identify the target products' structural characteristics. Excellent catalytic activity was demonstrated by the ZnO NPs, and the suggested approach is capable of producing the necessary compounds with good yield and purity.

**Shakeel Ahmed Ansari *et, al.*, (2011)** Reported the use of ZnO-NP for immobilisation of b- galactosidase revealed a stable and nontoxic enzyme-matrix association. Kinetic tests demonstrated a considerable boost in the enzyme's

stability and activity against pH, temperature, and product inhibition upon binding to nanoparticles, which could contribute to its improved use in many analytical, industrial, and therapeutic applications in the future. The method's applicability can be expanded further in the development of therapeutic medicines as innovative targeted drug delivery for lactose intolerant patients worldwide.

**Kodihalli *et.al.*, (2011)** Studied the synthesis of Zinc oxide (ZnO) nanoparticles of various sizes (20, 44, and 73 nm) were effectively synthesised in an undivided cell under galvanostatic mode at room temperature using an aqueous sodium bicarbonate electrolyte and sacrificial Zn anode and cathode. X-ray diffraction (XRD), X-ray photoelectron spectra (XPS), scanning electron microscopy, and energy dispersive analysis of X-ray were used to characterise the as-synthesized product. It was also discovered that photodegradation is affected by exposure time and dye solution pH. It was discovered that as-synthesized powder had good photocatalytic activity with 92% MB degradation, implying that ZnO nanoparticles can play an essential role as a semiconductor photocatalyst. Zinc Oxide; Methylene Blue; Photocatalytic activity; Semiconductor.

**Khorsand Zak *et.al.*, (2011)** Prepared zinc oxide nanoparticles (ZnO-NPs) were created using a solvothermal technique. The polymer agent TEA was used to stop the growth of ZnO-NPs. X-ray diffraction, transition electron microscopy, and field emission electron microscopy were used to analyse the ZnO-NPs. The solvothermal ZnO-NPs generated at 150°C for 18 hours had a hexagonal (wurtzite) structure, with a crystalline size of 33.2 nm and a particle size of 48.7 nm. The results show that TEA is an effective polymer agent for producing homogeneous ZnO-NPs.

**Xianyong Lu *et.al.*, (2011)** reported Sonochemical synthesis of Mg-doped ZnO nanoparticles. Scanning electron microscopy (SEM) and X-ray powder diffraction XRD used to evaluate the products. ZnO doped with Mg (II) nanoparticles and ZnO nanoparticles manufactured using the same approach all had spherical topography, according to SEM images. The doped nanoparticles had the same crystal structures as the pure ZnO nanoparticles, according to XRD patterns. The lattice volume of Mg-doped ZnO nanoparticles was greater than that of un-doped

nanoparticles. X-ray photoelectron spectroscopy (XPS) revealed not only the molar ratio of Mg and Zn elements on the surface of nanoparticles, but also their valence within nanoparticles. When compared to pure ZnO nanoparticles, Mg-doped ZnO nanoparticles demonstrated superior photocatalytic activities.

**Parthasarathi *et.al.*,(2011)** They discovered that ZnO-treated woven and knitted fabrics had high antibacterial activity against two representative bacteria: *Staphylococcus aureus* and *Klebsiella pneumoniae*. As a result, to avoid cross-infections, it is best suited for defence garments such as bed sheets, gloves, and T-shirts. This work presents a simple method for the aqueous preparation of ZnO nanocomposites and their application onto 100% cotton and 45/55% polyester/cotton fabrics to impart antibacterial property, with a reduction percentage of around 97% against *Staphylococcus aureus* and 98% for *Klebsiella pneumoniae* to control cross-infections for defence personnel in extreme climates.

**Qayyum Husain *et.al.*,(2011)** ZnO-NP bound galactosidase was found to be more stable against physical and chemical denaturants than soluble and native ZnO adsorbed galactosidase. As a result, reactors containing ZnO-NP adsorbed enzyme could be used for batch and continuous lactose hydrolysis in milk and whey in the near future. This type of nanomatrix could also be used as a carrier for enzyme immobilisation in other industrial applications. The method's applicability can be expanded in the development of therapeutic medicines as innovative targeted drug delivery for lactose-intolerant patients around the world.

**Nawaz *et.al.*, (2011)** They investigated the wet chemical approach of producing nanoscale zinc oxide from zinc nitrate and sodium hydroxide precursors. During retanning, nano-sized zinc oxide particles were applied to goat skin in the same way that control leather was. The resulting leather was tested for antibacterial activity using the diffusion method with *Bacillus subtilis*, *Escherichia coli*, and *Clostridium perfringens* bacteria. It has been discovered that nanozinc oxide suppresses bacterial development on leather without degrading its quality.

**Sricharussin *et.al.*,(2011)** ZnO in various shapes multi petals, rods, and spheres was manufactured and then put on cotton fabric for UV-blocking and anti-bacterial qualities. XRD and SEM were used to analyse the ZnO particles. The prepared suspension was applied to cotton fabrics using the pad-dry-cure method at 150 o C. SEM, XRD, and atomic absorption spectroscopy were used to evaluate the features of the fabric coating (AAS). The UV-blocking effectiveness was assessed using a UV-Vis spectrophotometer, and the antibacterial activity was determined using the AATCC 147 technique. The XRD and SEM measurements on the ZnO powders reveal that we can manufacture a variety of ZnO forms.

**Tugrul Yumak *et.al.*, (2011)** ZnO nanoparticles (ZNP) of around 30 nm size were synthesised by the hydrothermal method and studied using X-ray diffraction (XRD), Braun-Emmet-Teller (BET), N-2 adsorption analysis, and transmission electron microscopy (TEM). The researchers then developed ZnO nanoparticles supplemented with poly (vinylferrocenium) (PVF +) modified single-use graphite electrodes for electrochemical monitoring of Hepatitis B virus (HBV) nucleic acid hybridization. SEM was used to evaluate the surfaces of polymer-modified and polymer-ZnO nanoparticle-modified single-use pencil graphite electrodes (PGEs) (SEM). Following the optimization investigations, sequence-selective DNA hybridization was studied using a complementary amino-linked probe (the "target"), noncomplementary (NC) sequences, or a target and mismatch (MM) mixture in the ratio of (1:1).

**Elaheh *et.al.*,(2011)** This study describes a simple microwave method for producing zinc oxide nanoparticles (ZnONPs) using a green solvent, trihexyltetradecylphosphonium bis(trifluoromethyl)sulfonyl-imide To the best of our knowledge, there is no report of anynanoparticles being synthesised using this ionic liquid.Due to the low interface tension of trihexyltetradecylphosphonium bis(trifluoromethyl)sulfonyl-imide, it may increase the nucleation rate, favouring the formation of smaller ZnO-NPs. X-ray diffraction (XRD), transmission electron microscopy (TEM), and UV-vis spectroscopy were used to characterise the ZnONPs that were created. The hexagonal wurtzite structure of the ZnO-NPs is

shown by the XRD pattern. The remarkable crystallinity of the resultant nanoparticles is indicated by the great intensity and narrow width of the ZnO diffraction peaks.

**Sarmenio Saliba *et.al.*, (2011)** they described the fabrication of a new liquid crystal based on zinc oxide nanoparticles in this paper. Because of the presence of fluxional ligands, the hybridised material exhibits mesomorphic behavior even with a high inorganic concentration. It has intriguing luminous characteristics and could be used in electro-optical applications.

**Lian Zhen Li *et.al.*, (2011)** They investigated the ability of soil extracts to reduce the harmful effects of ZnO NPs on filter paper, which may be due to the presence of salts and organic carbon. The use of soil extract as a test medium in ecotoxicological assays can improve the prediction value of such filter paper tests for assessing NP environmental risk. Furthermore, when investigating the behaviour and transfer of NPs in soil ecosystems, the dissolving behaviour and potential toxicity of ZnO NPs must be examined to assess their particular dangers.

**Chen *et.al.*,(2011)** Due to its low cost, simplicity, and relatively low growing temperature, hydrothermal synthesis is of great interest (typically below 200 °C).The synthesis can also be risk-free and ecologically beneficial because it is carried out in aqueous solutions without the use of organic solvents (depending on precursor chemicals). As a result, it has been the focus of a lot of research lately. This article reviews current developments in the hydrothermal production of zinc oxide nanoparticles, focusing on their practical applicability for various uses.

**Rajendran *et.al.*,(2010)** has been proposed a study of the growing field of nanoscience and nanotechnology is the application of materials and structures with a typical size of 1 to 100 nanometers (nm).There is ongoing interest in the creation of noble metal nanoparticles for use in biology, electronics, textiles, electronics, and catalysis. Antimicrobial textiles have just come into existence as a result of increased awareness of personal hygiene, contact disease transmission, and general sanitation. The findings reveal that both qualitative and quantitative tests of the

finished fabric against *S. aureus* revealed strong antibacterial activity. ZnO nanoparticles were found to be embedded in the treated fabrics, according to the SEM examination. The treated fabric's wash durability study was also conducted, and it was discovered that it could endure up to 25 wash cycles.

**Engelbert Redel *et.al.*,(2010)** provided a simple sol-gel method for making colloiddally stable F ZnO nanoparticles in ROH, an alcoholic solvent. They demonstrate that as alkyl chain length and alcohol solvent branching are increased, ZnO nanoparticles (4-42 nm) grow monotonically in size.

These colloiddally stable and size-controllable metal oxide nanoparticles allow for the creation of photonic crystal multilayers and films with exceptional optical quality, and it has been discovered that these properties scale with the nature of the alcohol. The production of one-dimensional porous photonic crystals made of ncZnO/ncWO<sub>3</sub> multilayers, whose photonic stop band can be modified by adjusting nanoparticle size, serves as a demonstration of the usefulness of these colloiddally stable nanoparticles.

**Li Yun Yang *et.al.*,(2010)**. proposed a green technique for the manufacture of ZnO<sub>2</sub> nanoparticles based on the reaction between hydrozincite ( $Zn_5(CO_3)_2(OH)_6$ ) powder and hydrogen peroxide in aqueous solution at room temperature. X-ray diffraction, transmission electron microscopy, and Raman results showed that the end products were pure cubic phase ZnO<sub>2</sub> nanoparticles with diameters ranging from 3.1 to 4.2 nm. Thermogravimetric measurement revealed that between 180 and 350 °C, the as-synthesized ZnO<sub>2</sub> nanoparticles lost roughly 16.7% of their weight, which is commensurate with the theoretical quantity of O<sub>2</sub> released from ZnO<sub>2</sub> decomposition. The current technology was environmentally friendly, easy, and inexpensive, and it should be suited for large-scale manufacture of multifunctional ZnO<sub>2</sub> nanoparticles.

**Anita *et.al.*,(2010)** Studied the application of nano zinc oxide particles to cotton fabric confers the functional feature of antibacterial resistance. Antibacterial activity against *Staphylococcus aureus* was 99.99%, whereas antibacterial activity

against *Escherichia coli* was 80%. The nanoparticles are roughly 50 nm in size, according to the SEM study. The fabric's resistance to mechanical forces is visibly reduced, but not to the point where the fabric is deemed unusable for its original functions.

**Sween John *et.al.*,(2010)** The authors present a one-of-a-kind Zinc oxide (ZnO) Hydrogel fluorescent colloidal semiconductor nanomaterials system with potential bio-medical applications such as cell and tissue imaging. Arc discharge-produced ZnO nanoparticles (NPs) were coupled to a biocompatible polymer matrix based on poly N-isopropylacrylamide (PNIPAM). Hydrogel colloidal dispersion considerably improves the stability and fluorescence of ZnO nanoparticles. Photoluminescence spectroscopy shows that the fluorescence in the ZnO-hydrogel colloidal system is roughly 10 times higher than in the ZnO-water system, demonstrating the surface modification of ZnO nanoparticles by the hydrogel polymer matrix. The femtosecond time-resolved fluorescence measurement shows that the fluorescence is caused by an increase in absorption by ZnO nanoparticles due to scattering by PNIPAM nanospheres.

**Omid Zabihi *et.al.*,(2010)** They evaluated the curing, thermal degradation kinetics, and mechanical properties of epoxy resin based on bisphenol A diglycidyl ether, 2,2'-diamino-1,1'-binaphthalene as a hardener, and ZnO as a nanofiller. A percentage of ZnO nanoparticles of 5 phr resulted in better thermal and mechanical properties. The best-selected kinetic model was found to be a two-parameter autocatalytic model. Furthermore, the kinetic model's predicted curves fit well with the dynamic DSC thermograms. The addition of ZnO nanoparticles to the epoxy matrix increased its thermal stability and activation energy of thermal degradation significantly. When compared to clean epoxy, the epoxy nanocomposite had a higher storage modulus and glass transition temperature.

**Stephan Hackenberg *et.al.*,(2010)** They stated, "Despite the increasing use of zinc oxide nanoparticles (ZnO-NPs) in industrial applications, research on their potential hazardous characteristics is inconsistent. The current work compared the cytotoxicity and genotoxicity of ZnO-NPs to ZnO powder in primary human nasal

mucosa cells cultivated in an air-liquid interface. In addition, IL-8 secretion was assessed as a marker for pro-inflammatory effects. Transmission electron microscopy was used to examine particle shape and intracellular distribution (TEM). In addition, IL-8 secretion was assessed as a marker for pro-inflammatory effects. Transmission electron microscopy was used to examine particle shape and intracellular distribution (TEM).

**Prantik Banerjee *et.al.*,(2010)** Zinc oxide nanoparticles were produced sonochemically from a zinc acetate solution in aqueous methanol, ethanol, and isopropanol containing around 5% alcohol. Characterization with FESEM, XRD, AFM, and BET surface areas reveals that the produced particles varied in form and size. The most crystalline ZnO was found to be that synthesised with isopropanol. The nanoparticles created were used in the photocatalytic reduction of hexavalent chromium in an aqueous medium using solar radiation. The initial reduction rates were found to vary with the shape of ZnO crystallites.

**Yoshiaki Hattori *et.al.*,(2010)** They stated A zinc electrode is efficiently synthesised into nanoparticles by microwave plasma in liquid. The alcohol-based nanoparticles produced pure zinc particles in the shape of spheres or hexagonal cylinders at a rate of 3.3 g/h with an energy consumption of 267 J/mg for 1 mg. In contrast, nanoparticles formed in pure water are made up of Zn and ZnO. Through heat or the passage of time, Zn interacts with water to form ZnO, which emits hydrogen gas. An upper disc placed 1 mm away from the electrode, together with bubbles formed concurrently with plasma ignition, are critical in the production of nanoparticles.

**Ahmeda Tayel *et.al.*,(2010)** The present proliferation of nanomaterial applications encourages the quest for other conceivable functionalities of these tiny particles. The antibacterial potentiality of zinc oxide (ZnO) nanoparticles (NPs) over standard ZnO powder was assessed using qualitative and quantitative testing against nine bacterial species, predominantly foodborne pathogens. As an antibacterial agent, ZnO NP outperformed powder.

**Sushil Kumar Kansal *et.al.*,(2010)** In the current study, a simple hydrothermal approach without any catalysts, templates, or substrates was used to create a ZnO nanostructure that resembles a flower. By using XRD, SEM, and TEM, the phase structure and morphology of the synthesised ZnO have been identified. The diffuse reflectance spectra (DRS), FT-IR spectra, BET surface area, and photoluminescence (PL) at room temperature have also been studied. The use of the produced ZnO as a photocatalyst for the decolorization of pararosaniline chloride dye and its simulated dyebath effluent was also examined. The comparison of the photocatalytic activity of synthetic and commercial ZnO has now been completed. Moreover, experiments were conducted to examine the stability and reusability of the synthesised ZnO.

**Slama *et.al.*(2010)** By using the sol-gel process and supercritical drying in ethyl alcohol at 250°C, vanadium-doped zinc oxide nanoparticles have been created. The produced nanopowder was examined using a variety of methods, including particle size analysis, scanning electron microscopy (SEM), transmission electron microscopy (TEM), X-ray diffraction (XRD), and photoluminescence, after being heated at 500 °C for two hours in a natural atmosphere (PL). A significant luminescence band in the visible range is present in the powder's as-prepared form, which has an average particle size of 25 nm. The energy location of the PL band that results from photoluminescence excitation (PLE) depends on the excitation wavelength, and this PL can be produced by a few visible excitations.

**Rekha *et.al.*,(2010)** By using the co-precipitation technique, polycrystalline ZnO doped with Mn (5 and 10 at%) was created. Researchers looked at the impact of Mn doping on the photocatalytic and antibacterial activities as well as the effect of doping concentration on the structural and optical characteristics of nanoparticles. The Wurtzite structure of ZnO has not changed as a result of the substitution of the Mn 2 + ions for the Zn 2 + ions, according to the structural and optical characteristics of the particles. With rising dopant concentration, the optical spectra revealed a blue shift in the absorbance spectrum.

Methylene blue (MB) degradation in water under the UV region was used to gauge the photocatalytic activity of ZnO particles. It was discovered that when exposed to UV light, undoped ZnO bleaches MB significantly more quickly than manganese doped ZnO.

**Rooma Devi *et.al.*,(2010)** Without the need for a calcination step, zinc oxide nanoparticles (ZnO-NPs) were produced from zinc nitrate using an easy and effective technique in aqueous medium at 55 °C. A ZnO-NPs-polypyrrole (PPy) composite film was created by electropolymerizing a combination of pyrrole and ZnO-NPs on a Pt electrode. By physisorption, Xanthine Oxidase (XOD) was immobilised on this nanocomposite film. Fourier transform infrared (FTIR), cyclic voltammetry (CV), X-ray diffraction (XRD), scanning electron microscopy (SEM), transmission electron microscopy (TEM), and electrochemical impedance spectroscopy (EIS) were used to characterise the ZnO-NPs/polypyrrole/Pt electrode before and after immobilisation of XOD. The xanthine oxidase Michaelis Menten constant ( $K_m$ ) was 13.51 M and the  $I_{max}$  was 0.071 A.

**Khizar Hayat *et.al.*,(2010)** Using the use of improved sol gel and precipitation techniques, zinc oxide nanoparticles were created. By adjusting the temperature from 400 to 700 C, the impact of calcination temperature on the shape and crystallite size of ZnO was investigated. X-ray diffraction (XRD), field emission scanning electron microscopy (FESEM), energy dispersive X-ray spectroscopy (EDXS), and transmission electron microscopy were used to analyse the nano-structured ZnO particles (TEM). To maximise PCD phenol, many other parameters, including photocatalyst concentration, initial pH, and initial phenol concentration, were also studied in addition to the effect of calcination temperature. The operating parameters reflect the anticipated influence on the photocatalytic degradation process' efficiency. The outcomes are consistent with the pseudo-first order rate kinetics.

**Saji George *et.al.*,(2010)** They looked examined the impact of zinc oxide nanoparticles (nano-ZnO) on the roots of rice (*Oryza sativa* L.). In this study, the percentage of germination of seeds, the length of the roots, and the total number of roots are all studied. The findings indicate that the percentage of seeds that

germinate is unaffected; nevertheless, rice roots are seen to be adversely affected by nano-ZnO in the early seedling stage. It has been discovered that nano-ZnO shortens and fewer roots. This study highlights the need for environmentally sound waste disposal of nanoparticle-containing wastes, highlights the need for additional research on the effects of nanoparticles on agricultural and environmental systems, and demonstrates that direct exposure to specific types of nanoparticles causes significant phytotoxicity.

**Ahmed A.Tayel *et.al.*,(2010)** The present proliferation of nanomaterial applications encourages the investigation of further potential uses for these tiny particles. Using qualitative and quantitative tests, the antibacterial potentiality of zinc oxide (ZnO) nanoparticles (NPs) against nine bacterial species, largely foodborne including pathogens, was assessed in comparison to standard ZnO powder. As an antibacterial agent, ZnO NP proved more effective than powder. In general, Gram-positive bacteria are more susceptible to ZnO than Gram-negative bacteria. When *Staphylococcus aureus* and *Salmonella typhimurium* were exposed to their respective least inhibitory concentrations of ZnO NP, the number of cells fell to zero within 8 and 4 hours, respectively.

**Tugrul Yumak *et.al.*,(2010)** In their work, ZnO nanoparticles (ZNP) of about 30 nm in size were produced by the hydrothermal technique and examined using transmission electron microscopy, Braun-Emmet-Teller (BET), N<sub>2</sub> adsorption analysis, and X-ray diffraction (TEM). Next, single-use graphite electrodes enhanced with ZnO nanoparticles enriched with poly (vinylferrocenium) (PVF<sup>+</sup>) were created for the electrochemical monitoring of nucleic acid hybridization associated to the hepatitis B virus (HBV). Initially, scanning electron microscopy (SEM) was used to evaluate the surfaces of polymer modified and polymer-ZnO nanoparticle modified single-use pencil graphite electrodes (PGEs) (SEM). After that, the modified PGEs based on polymer-ZnO nanoparticles were assessed for the electrochemical detection of DNA based on changes in the guanine oxidation signals.

**Rooma Devi *et.al.*,(2010)** Without the need for a calcination step, zinc oxide nanoparticles (ZnO-NPs) were produced from zinc nitrate using an easy and effective technique in aqueous medium at 55 °C. A ZnO-NPs-polypyrrole (PPy) composite film was created by electropolymerizing a combination of pyrrole and ZnO-NPs on a Pt electrode. By physisorption, Xanthine Oxidase (XOD) was immobilised on this nanocomposite film. Fourier transform infrared (FTIR), cyclic voltammetry (CV), X-ray diffraction (XRD), scanning electron microscopy (SEM), transmission electron microscopy (TEM), and electrochemical impedance spectroscopy (EIS) were used to characterise the ZnO-NPs/polypyrrole/Pt electrode before and after immobilisation of XOD. A potentiostat was used to link the working electrode (XOD/ZnO-NPs-PPy/Pt), reference electrode (Ag/AgCl), and accessory electrode (Pt wire) of a xanthine biosensor.

**Renata Marczak *et.al.*,(2009)** A simple colloidal approach was used to synthesise ZnO nanoparticles in ethanol. Temperature, as well as the presence of the chemical byproduct lithium acetate, were discovered to influence particle growth during the ageing process. This process might be nearly totally stopped by removing this byproduct through repeated flocculation of the ZnO particles with n-heptane. Steady-state absorption spectroscopy, as well as steady-state and time-resolved emission tests, confirmed a connection between the ZnO and dye molecules, as well as electron injection into the ZnO. The findings of this work pave the way for the development of organised ZnO-based nanostructures capable of efficiently harvesting light energy.

**Ashok Kumar *et.al.*,(2009)** According to their study, the ZnO composite modified electrode has better electrocatalytic activity for glucose oxidation. The obtained results demonstrated that glucose determination can be easily conducted using the ZnO composite films, and the modified electrode exhibited significantly increased electrocatalytic activity towards glucose with good stability in solution. SEM, AFM, EIS, and CV were used to characterise the ZnO composite films. The newly created non-enzymatic glucose sensor has a variety of appealing characteristics, including high sensitivity, stability, repeatability, selectivity, and fast response. The

method's application to the determination of glucose in human urine samples was demonstrated.

**Renata Marczak *et.al.*, (2009)** A simple colloidal approach was used to synthesise ZnO nanoparticles in ethanol. Temperature, as well as the presence of the chemical byproduct lithium acetate, was discovered to influence particle growth during the ageing process. This process might be nearly totally stopped by removing this byproduct through repeated flocculation of the ZnO particles with n-heptane. Steady-state absorption spectroscopy, as well as steady-state and time-resolved emission tests, confirmed a connection between the ZnO and dye molecules, as well as electron injection into the ZnO. The findings of this work pave the way for the development of organised ZnO-based nanostructures capable of efficiently harvesting light energy.

**Ashok Kumar *et.al.*, (2009)** According to their study, the ZnO composite modified electrode has better electrocatalytic activity for glucose oxidation. The obtained results demonstrated that glucose determination can be easily conducted using the ZnO composite films, and the modified electrode exhibited significantly increased electrocatalytic activity towards glucose with good stability in solution. SEM, AFM, EIS, and CV were used to characterise the ZnO composite films.

The newly created non-enzymatic glucose sensor has a variety of appealing characteristics, including high sensitivity, stability, repeatability, selectivity, and fast response. The method's application to the determination of glucose in human urine samples was demonstrated.

**Latha Kumari *et.al.*, (2009)** Zinc oxide (ZnO) spherical nanoparticles (SNPs) and bitter-melon-like (BML) microparticles were synthesized by a hydrothermal route using a zinc (Zn) plate as a source and substrate at various synthesis conditions. The structural analysis confirmed the formation of ZnO with hexagonal wurtzite phase on the hexagonal Zn substrate with growth of the ZnO microparticles along the [1 0 1] direction. The UV-Vis absorption spectra of the ZnO microparticles indicated absorption peaks in the UV region which can be attributed to the band gap of ZnO.

The room temperature photoluminescence (PL) of the ZnO microparticles exhibited a broad emission band, which is fitted with four Gaussian peaks and were assigned to transitions involving free excitons and various defect centers. The growth model for the formation of ZnO micro- and nanoparticles is presented.

**Malhotra *et.al.*,(2009)** In a dense plasma focus (DPF) device's post-focus phase, luminescent ZnO nanoparticles have been created on silicon and quartz substrates under severely non-equilibrium conditions of intense ion condensation. Ar +, O +, Zn +, and ZnO + ions are produced as a result of the interaction between the surfaces of the ZnO pellets at the anode and the hot, concentrated argon plasma focus. On Si(1 0 0) and quartz substrates, it is discovered that the sizes, structural makeup, and photoluminescence (PL) characteristics of the ZnO nanoparticles appear to be considerably different. The size of the ZnO nanoparticles, which vary from 5-7 nm on Si(1 0 0) substrates to 10-38 nm on quartz substrates, is crystalline, according to the results of x-ray diffractometry and atomic force microscopy.

**Bajpai *et.al.*,(2009)** They looked at how well chitosan sheets absorbed moisture as part of their study. It is discovered that the experimental moisture uptake data obtained at 10, 25, and 37°C fit the GAB isotherm model quite well. It is discovered that the water vapour permeability rises with temperature. The water vapour permeability is improved by the application of plasticizer. The films have also undergone X-ray diffraction, differential scanning calorimetry, surface plasma reflectance, and scanning electron microscopy investigations after being loaded with ZnO nanoparticles.

Scherrer's equation reveals that the crystal's size is approximately 15 nm. Size, aggregation, shape, dissolution, and surface characteristics of ZnO NPs were identified. In the seawater exposure medium, ZnO NPs underwent aggregation and partial dissolution, resulting in a size distribution with a range from discrete nanoparticles to the biggest aggregate of several micrometres.

**Rahman Hallaj *et.al.*,(2008)** The author described electrodeposited zinc oxide (ZnO<sub>x</sub>) nanoparticles on the surface of a glassy carbon (GC) electrode using a

potential step of 0.8 V for 120 s from a zinc acetate solution at 50 C. The guanine was then oxidised by potential cycling, resulting in an electroactive redox pair that was strongly and irreversibly adsorbed on the ZnOx nanoparticles/modified electrode. At pH 2–12, the modified electrode demonstrates a pair of well-defined, almost reversible, and surface-controlled redox couples. The surface coverage ( $\Gamma$ ) and heterogeneous electron transfer rate constant ( $k_s$ ) of the adsorbed redox couple were approximately  $9.5 \times 10^{-9}$  mol cm<sup>-2</sup> and 3.18 (0.20) s<sup>-1</sup>, respectively, indicating a high loading ability of ZnOx nanoparticles towards the guanine oxidation product and a great facilitation of electron.

**Ravindra P. Singh *et.al.*,(2007)** Here, they presented a brand-new biological method for producing zinc oxide (ZnO) nanoparticles at room temperature using Maddar (*Calotropis procera*) latex. The production of ZnO nanoparticles is revealed by the X-Ray Diffraction (XRD) pattern, which demonstrates crystallinity. The size and form of the particles were estimated by transmission electron microscopy (TEM) to be between 5 and 40 nm. The particles are round and granular, according to an image from a scanning electron microscope (SEM). ZnO nanoparticles exhibit a distinctive absorption peak during UV-Vis absorption. Studies on photoluminescence (PL) were carried out to highlight its emission characteristics.

# *Materials and Methods*

## **3.METHODS AND METHODOLOGY**

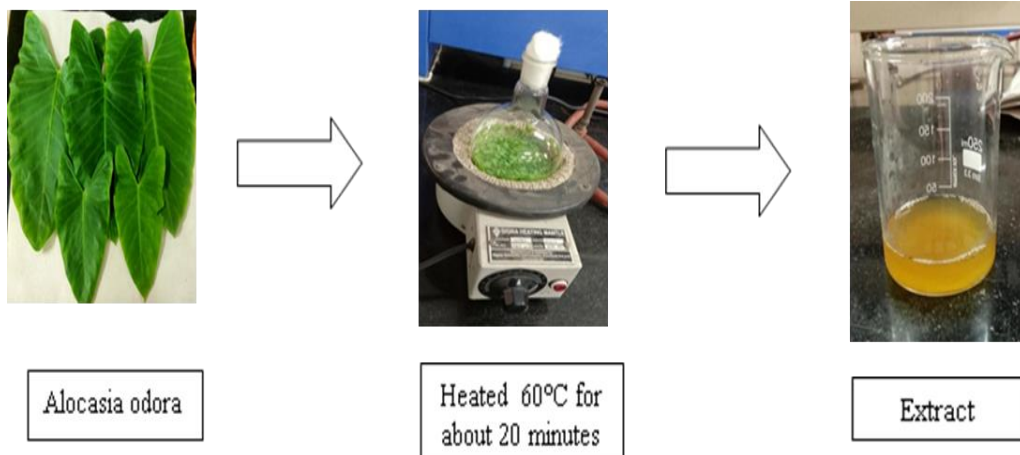
### **3.1Materials**

Zinc oxide nanoparticles were synthesized through two methods, the first one is through Chemical method and the second one is green synthesis using plant extract. Zinc oxide, starch and sodium hydroxide were used for chemical synthesis and zinc acetate dihydrate, Plant extract, sodium hydroxide and ethanol were used for green synthesis *Alocasia odora* leaves were collected from our university campus and confirmed the leaves with the help of botany department. The leaves were dried in shade for 1 week.

### **3.2 Synthesis of ZnO nanoparticles**

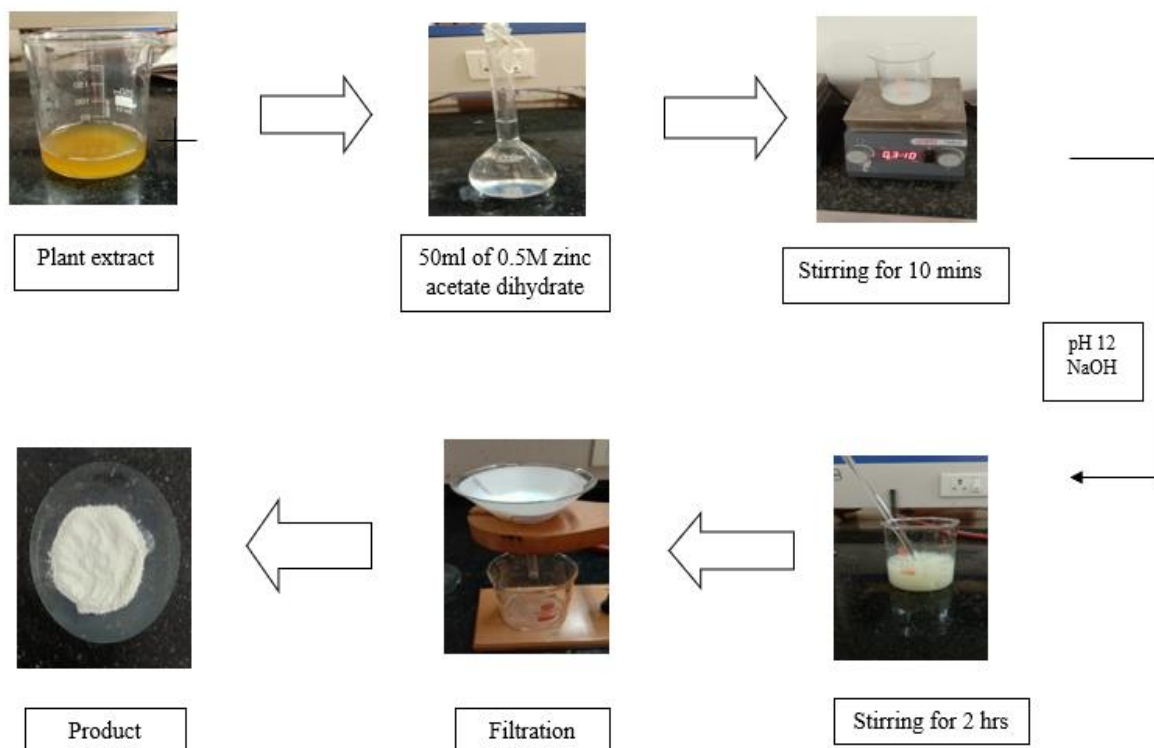
#### **Green synthesis**

Fresh leaves of *Alocasia odora* were thoroughly cleaned with running tap water to remove debris and other contaminants, followed by distilled water and air dried at room temperature. Leaves were finely chopped into small pieces. The aqueous extract of sample was prepared by boiling the freshly collected cut leaves (10g), with 100 ml of distilled water, at 60°C for about 20 minutes, until the color of the aqueous solution changes from watery to light brown. Then the extract was cooled to room temperature and filtered using Whatman filter paper. The extract was stored in a refrigerator in order to be used for further experiments.



### 3.3 ZnO-NPs Synthesis from plant extract

For the synthesis of ZnO nanoparticles, 50ml of 0.5M zinc acetate dihydrate solution was prepared using distilled water. 1ml of aqueous leaf extract was introduced into the above solution. After 10 minutes stirring. In order to maintain the pH 12 NaOH solution was added drop by drop, which resulted in a pale white aqueous solution. This was then placed in a magnetic stirrer for 2 hrs. The pale white precipitate was then taken out and washed over and over with distilled water and then with ethanol to remove impurities. Then a pale white powder of ZnO nanoparticles was obtained after drying in the oven.



### 3.4 Phytochemical screening :

Phytochemical examinations were carried out for the extract as per standard methods (Tiwari *et al.*, 2011)

1. **Detection of alkaloids:** Extracts were dissolved individually in distilled water and filtered.

**a)Mayer's Test:** Filtrates were treated with Mayer's reagent (Potassium Mercuric Iodide). Formation of a yellow coloured precipitate indicates the presence of alkaloids.

**b)Wagner's Test:** Filtrates were treated with Wagner's reagent (Iodine in Potassium Iodide). Formation of brown/reddish precipitate indicates the presence of alkaloids.

**c) Dragendorff's Test:** Filtrates were treated with Dragendorff's reagent (solution of Potassium Bismuth Iodide). Formation of red precipitate indicates the presence of alkaloids.

**d) Hager's Test:** Filtrates were treated with Hager's reagent (saturated picric acid solution). Presence of alkaloids confirmed by the formation of yellow coloured precipitate.

**2. Detection of carbohydrates:** Extracts were dissolved individually in 5 ml distilled water and filtered. The filtrates were used to test for the presence of carbohydrates.

**a) Molisch's Test:** Filtrates were treated with 2 drops of alcoholic  $\alpha$ -naphthol solution in a test tube. Formation of the violet ring at the junction indicates the presence of Carbohydrates.

**b) Benedict's Test:** Filtrates were treated with Benedict's reagent and heated gently. Orangered precipitate indicates the presence of reducing sugars.

**c) Fehling's Test:** Filtrates were hydrolyzed with dil. HCl, neutralized with alkali and heated with Fehling's A & B solutions. Formation of red precipitate indicates the presence of reducing sugars.

**3. Detection of glycosides:** Extracts were hydrolyzed with dil. HCl, and then subjected to test for glycosides.

**a) Modified Borntrager's Test:** Extracts were treated with Ferric Chloride solution and immersed in boiling water for about 5 minutes. The mixture was cooled and extracted with equal volumes of benzene. The benzene layer was separated and treated with ammoniacal solution. Formation of rose-pink colour in the ammoniacal layer indicates the presence of anthranol glycosides.

**b) Legal's Test:** Extracts were treated with sodium nitroprusside in pyridine and sodium hydroxide. Formation of pink to blood red colour indicates the presence of cardiac glycosides.

#### **4. Detection of saponins**

**a) Froth Test:** Extracts were diluted with distilled water to 20ml and this was shaken in a graduated cylinder for 15 minutes. Formation of 1 cm layer of foam indicates the presence of saponins.

**b) Foam Test:** 0.5 gm of extract was shaken with 2 ml of water. If foam produced persists for ten minutes it indicates the presence of saponins.

#### **5. Detection of phytosterols**

**a) Salkowski's Test:** Extracts were treated with chloroform and filtered. The filtrates were treated with few drops of Conc. Sulphuric acid, shaken and allowed to stand. Appearance of golden yellow colour indicates the presence of triterpenes.

**b) Libermann Burchard's test:** Extracts were treated with chloroform and filtered. The

filtrates were treated with few drops of acetic anhydride, boiled and cooled. Conc. Sulphuric acid was added. Formation of the brown ring at the junction indicates the presence of phytosterols.

#### **6. Detection of phenols**

**Ferric Chloride Test:** Extracts were treated with 3-4 drops of ferric chloride solution. Formation of bluish black colour indicates the presence of phenols.

#### **7. Detection of tannins**

**Gelatin Test:** To the extract, 1% gelatin solution containing sodium chloride was added. Formation of white precipitate indicates the presence of tannins.

#### **8. Detection of flavonoids**

**a) Alkaline Reagent Test:** Extracts were treated with few drops of sodium hydroxide solution. Formation of intense yellow colour, which becomes colourless on addition of dilute acid, indicates the presence of flavonoids.

**b) Lead acetate Test:** Extracts were treated with few drops of lead acetate solution. Formation of yellow colour precipitate indicates the presence of flavonoids.

### **9. Detection of proteins and amino acids**

**a) Xanthoproteic Test:** The extracts were treated with few drops of conc. Nitric acid. Formation of yellow colour indicates the presence of proteins.

**b) Ninhydrin Test:** To the extract, 0.25% w/v Ninhydrin reagent was added and boiled for a few minutes. Formation of blue colour indicates the presence of amino acid.

### **3.5 Characterization**

The characterization of ZnO NPs was carried out using the methods

- UV-Visible analysis
- FT-IR analysis
- SEM
- EDX
- 3D optical spectroscopy profilometry
- TGA analysis
- Antibacterial
- X-Ray diffraction

## **Characterization of Nanoparticles**

Characterization of nanoparticles was done by different methods. UV-visible spectral analysis was used to analyse the absorbance, Fourier transform infrared spectroscopy (FT-IR) gives specific signals for NPs. Shape of the nanoparticle were characterized by scanning electron microscopy, thermo gravimetric analysis, X-Ray diffraction.

### **UV-visible analysis**

UV-visible spectroscopy is usually conducted to confirm the synthesis of ZnO NPs. Peaks, which studied in the range of 200-400 nm. Different peaks are obtained in this range. Absorbance also obtained through this analysis. Conducting electrons start oscillating at a certain wavelength range due to surface Plasmon resonance. (Santhosh Kumar *et al.*, 2017)

### **FT-IR analysis**

Specific signals obtained by IR spectroscopy according to the vibrations of the molecule. FT-IR spectra and functional groups involved in ZnO NPs synthesis illustrated peaks in the range of 500-4000 $\text{cm}^{-1}$ . The sample pellet was placed into the sample holder and FT-IR spectra were recorded in FT-IR spectroscopy.

### **SEM Analysis**

SEM analysis is used to visualize the shape and size of nanoparticles. Scanning electron microscopy was adjusted in different magnifications and used to determine the shape of ZnO NPs. SEM images in different magnification ranges can be evaluated. (Santhosh Kumar *et al.*, 2017).

SEM image was usually used to study the morphology of synthesized nanoparticles (Kalpana handore. *et al.*, 2014)

### **3D Optical Profilometry**

LASER and AFM analyses have given us insight about the topography, roughness of nanoparticles. LASER imaging was conducted in different magnification range images clearly demonstrating smooth nanoparticles with capping of phytochemicals over the surface of nanoparticles (Santhosh Kumar j. *et al.*, 2017).

### **Thermo gravimetric analysis**

TGA is a method of thermal analysis in which changes in physical and chemical properties of materials are measured as a function of increasing temperature or as a function of time with constant temperature. It is a temperature based study.

### **X-Ray Diffraction**

XRD finds the geometry or shape of a molecule using X-rays. XRD techniques are based on the elastic scattering of X-rays from structures that have long range order. The X-rays get diffracted by a crystal because the wavelength of X-rays is similar to the inter-atomic spacing in the crystals

### **Anti-microbial activity studies**

A minimum of three to five colonies with the same morphological type that are well-isolated are chosen from an agar plate culture. Each colony's top is touched with a loop to transfer the growth into a tube holding 4 to 5 cc of an appropriate broth medium, such as Nutrient broth. Until the turbidity is reached or exceeded,

the broth culture is incubated at 35°C (usually 2 to 6 hours). To achieve turbidity, sterile saline or broth is added to the actively growing broth culture to regulate the turbidity. In the end, a suspension with 1 to 2 x 10<sup>8</sup> CFU/ml of *Staphylococcus aureus*, *Bacillus subtilis*, *Escherichia coli*, and *Pseudomonas aeruginosa* is produced. Both gramme positive and gramme negative bacteria were tested for ZnO NPs' antibacterial activity. The exact mechanism by which the nanoparticles were able to penetrate the bacteria is unknown, but research suggests that when bacteria were exposed to ZnO particles, their morphology changed, significantly increasing their permeability and interfering with the proper transport of the particles through the plasma membrane. The heightened surface reactivity, reduced particle size, increased specific surface area, and abrasive surface texture or surface defect of the synthesised NPs provide them their antifungal, anticorrosive, and antibacterial characteristics. The zone of inhibition attained using nanoparticles was significantly higher than the one attained using a normal disc, demonstrating the need for additional nanoparticle engineering to produce the desired effect. As a result, it is possible to claim that the zinc oxide nanoparticles are microbial growth in in-vitro antibacterial activity.

# *Results and Discussion*

## 4. RESULTS AND DISCUSSION

The results of the present work entitled “**Plant-mediated green synthesis of zinc oxide nanoparticles from *Alocasia odora* leaves**” discussed below.

### 4.1 Qualitative Phytochemical Analysis

The phytochemical analysis of the plant extract of *Alocasia odora* leaves is shown in table no 4.1. The analysis revealed the presence of several phytochemicals such as carbohydrates, alkaloids, glycoside, phenolic test, tannins, Saponins, flavonoids, phytosterols, proteins, and amino acids. The result + sign represents that positive, ++ indicates highly positive and – sign represents that absence of compounds.

S.No.	Chemical constituent	Phytochemicals Test	Result
1	Carbohydrates	Fehling's test	-
		Molisch's test	-
2	Alkaloids	Drangendroff's test	+
3	Glycoside	Legal's test	-
4	Phenolic test	Ferric chloride test	+
5	Tannins	Gelatin test	-
6	Saponins	Foam test	+
7	Flavonoids	Alkaline reagent test	-
8	Phytosterols	Salkowski's test	-
9	Proteins	Xanthoproteic test	-
10	Amino acid	Ninhydrin test	-

**Table: 4.1.1 Phytochemical constituents of *Alocasia Odora* leaf extract**



**Figure: 4.1.1 Preliminary phytochemical screening**

The presence of these compounds indicate the plant extracts are capable of acting as effective bioreductant

#### **4.2 Characterization**

The characterization of ZnO NPs was carried out using the methods

- UV-Visible analysis
- FT-IR analysis
- SEM
- EDX
- 3D optical spectroscopy profilometry
- TGA analysis
- Antibacterial
- X-Ray diffraction

## UV- visible spectroscopy

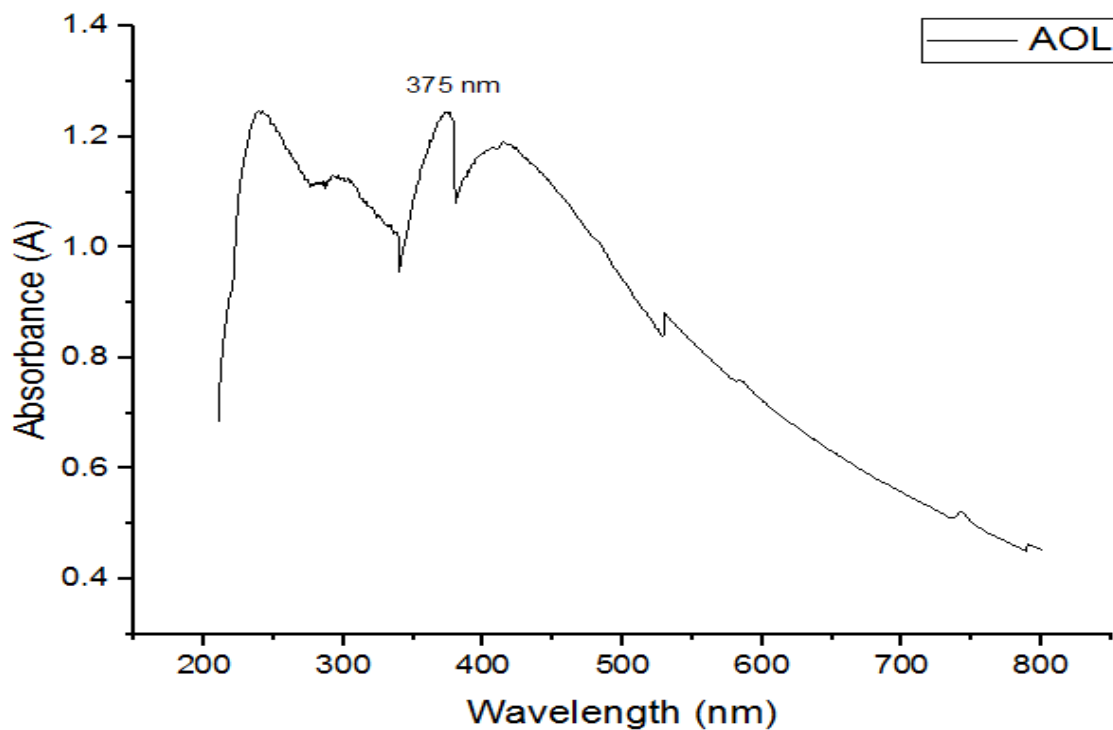


**Figure: 4.2.1 UV Spectrum of Green synthesized ZnO**

UV-Visible spectrophotometric analysis of synthesized ZnO nanoparticles is shown in the figure 4.2.1. An absorbance peak at 375 nm indicates the presence of ZnO nanoparticles, which is in accordance of UV absorbance result shown by previous studies. (Awwadet.al.,2014)

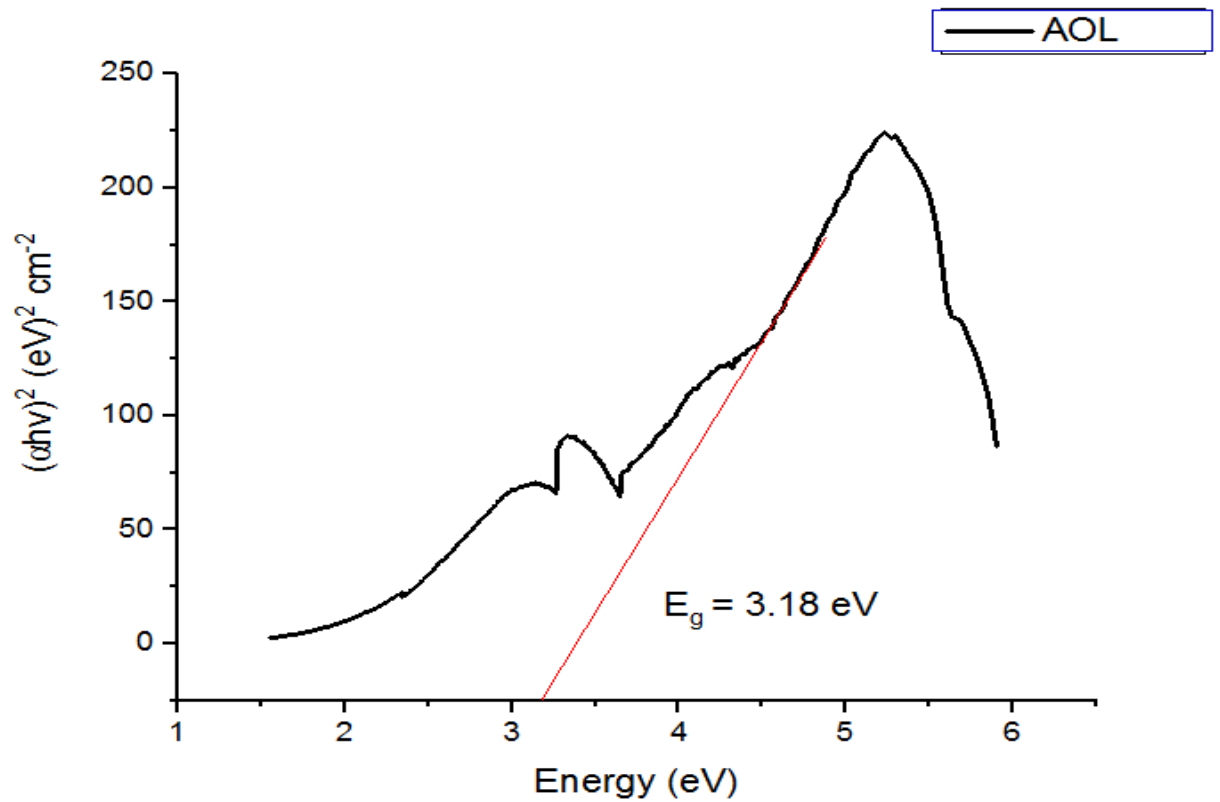


**Figure: 4.2.2 Tauc plot of ZnO-NPs**

The optical band gap of ZnO-NPs was calculated from UV-Visible spectra by the following as equation as  $\alpha = c (h\nu - E_{\text{bulk}})^{1/2} / h\nu$ . Figure 4.2.2 shows the plot drawn between  $h\nu$  versus  $(\alpha h\nu)^2$  for the formed ZnO NPs, by using UV-Visible Spectroscopy. The band gap was obtained by the exploration of a linear regression to x-axis in the plot and the gap was found to be 3.18 eV. The results confirmed by using aqueous leaf extracts of *Alocasia odora*. (Sireesh Babu Maddinedi *et.al.*,2020)

## FT-IR SPECROSCOPY

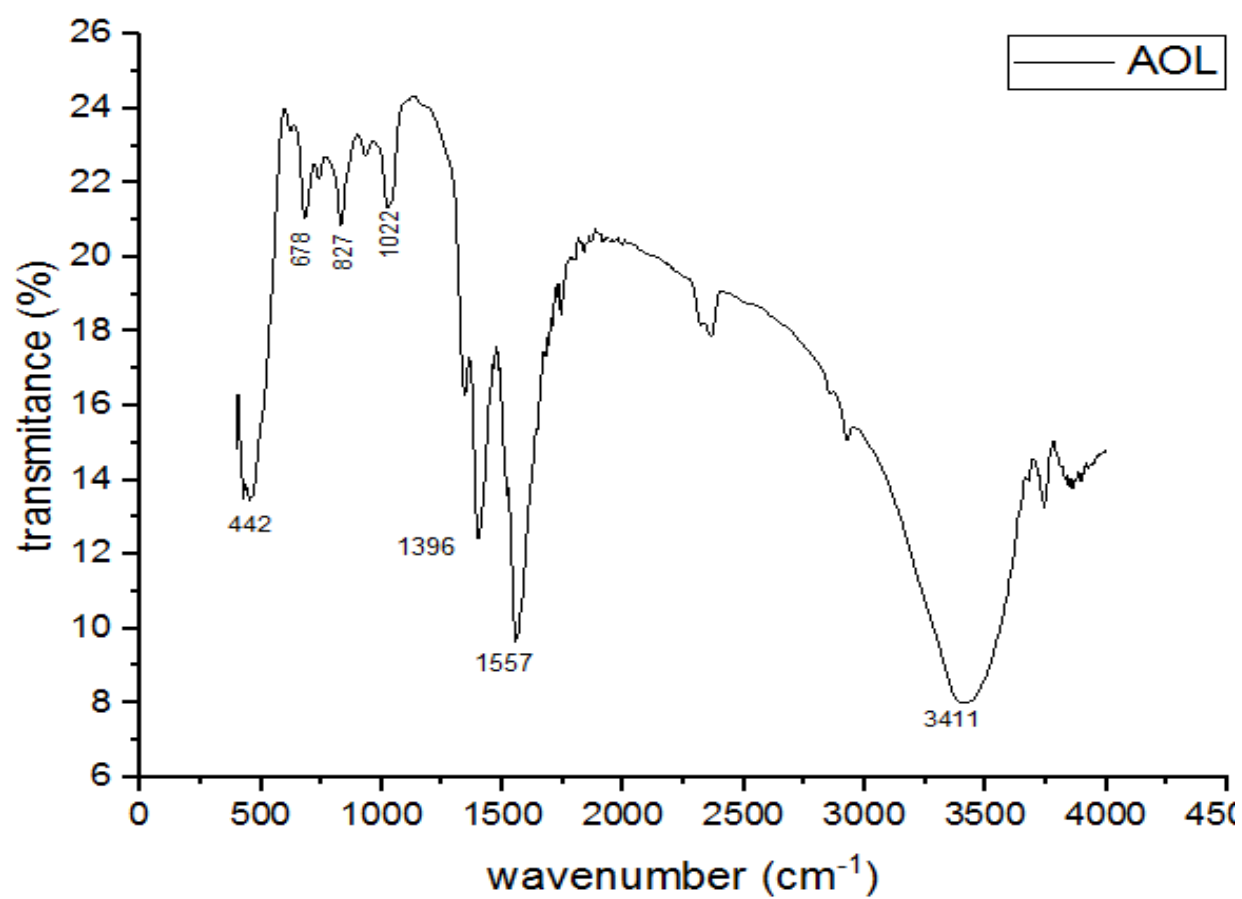


Figure: 4.2.3 FTIR image of ZnO NPs

Vibrational frequency $\text{cm}^{-1}$	Functional group	Reference
3411	O-H Stretching	Menazea <i>et.al.</i> ,(2021)
1396	O-H Stretching	Menazea <i>et.al.</i> ,(2021)
1022	-N-H, -C-O, -C-H	Maqsood Ahmad Malik <i>et.al.</i> ,(2021)
1551	H-OH	Bassant Naiel <i>et.al.</i> ,(2022)
442,678	Formation of ZnO NPs	Menazea <i>et.al.</i> ,(2021)
827	Metal oxygen bond	Ramachandran Ishwarya <i>et.al.</i> ,(2017)

**Table: 4.2.1 FT-IR Spectral range and functional group of ZnO NPs**

The synthesized Zinc oxide nanoparticles from leaf extract of *Alocasia odora* were analysed by FTIR spectroscopy in order to find the functional group present in the particles the bands at  $442\text{ cm}^{-1}$ ,  $678\text{ cm}^{-1}$  confirmed the presence of ZnO NPs which are attributed to Zn–O bond (Menazea *et.al.*,2021). The broad peak  $1396\text{ cm}^{-1}$  (Menazea *et.al.*,2021) corresponding to the presence of C-C stretching. The bonds appear  $827\text{ cm}^{-1}$  related to metal oxygen bond (Ramachandran Ishwarya *et.al.*,2017) and the peak at  $3411\text{ cm}^{-1}$  reveal in the presence of C-H stretching vibration of an aromatic aldehyde Menazea *et.al.*,2021). A peak at  $1022\text{ cm}^{-1}$  can be attributed to the C-O stretching of the primary alcohol Maqsood Ahmad Malik *et.al.*,2021). A peak around  $1551\text{ cm}^{-1}$  could be due to N-O stretching nitro group. These confirm the influence of phyto constituents on synthesis of ZnO nanoparticles. ( Bassant Naiel *et.al.*,2022)

## SCANNING ELECTRON MICROSCOPY

SEM was used to examine the size, shape, and composition of the produced ZnO nanoparticles. Figure illustrates the same, with particles that were synthesized in the same form and with an average size of 1  $\mu\text{m}$ . Due to the high surface energy of ZnO-NPs which typically occurs when synthesis is carried out in an aqueous medium and the limited space between particles caused by densification, proper aggregation is also observed. (Sadhan Kumar Chaudhuri *et.al.*,2017)

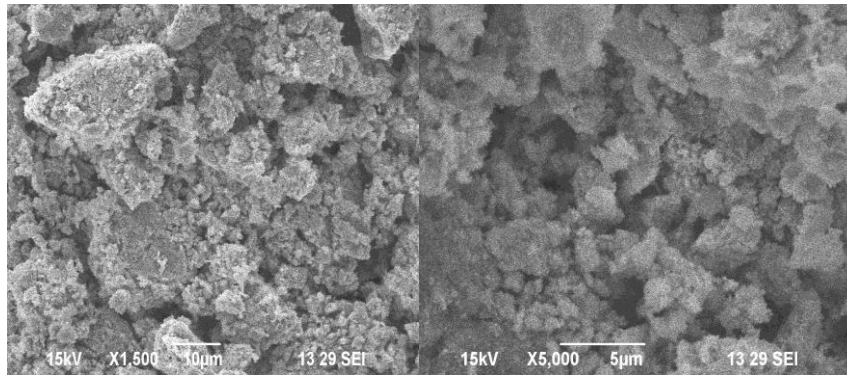


**Figure: 4.2.4 SEM images of ZnO NPs**

## ENERGY DISPERSIVE X-RAY ANALYSIS

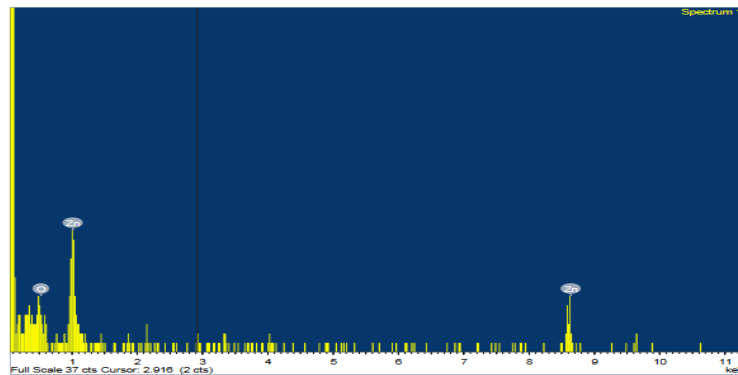


**Figure: 4.2.5 EDAX image of ZnO-NPs**

To understand the element composition of the produced ZnO nanoparticles, an Energy Dispersive X-Ray Diffraction (EDAX) research was conducted. EDAX images confirm the presence of the element zinc and oxygen signals. This research revealed that the peaks corresponded to the manufactured nanoparticle's optical absorption.

<b>Element</b>	<b>Weight %</b>	<b>Atomic %</b>
O	0.03	34.83
Zn	0.21	65.17

**Table: 4.2.2 EDAX Value of ZnO-NPs**

### **3D Optical Profilometer images of Green synthesized ZnO**

The topography and roughness of nanoparticles are revealed through optical profilometer studies. Pictures made it very evident how smooth nanoparticles were due to phytochemicals covering their surface.

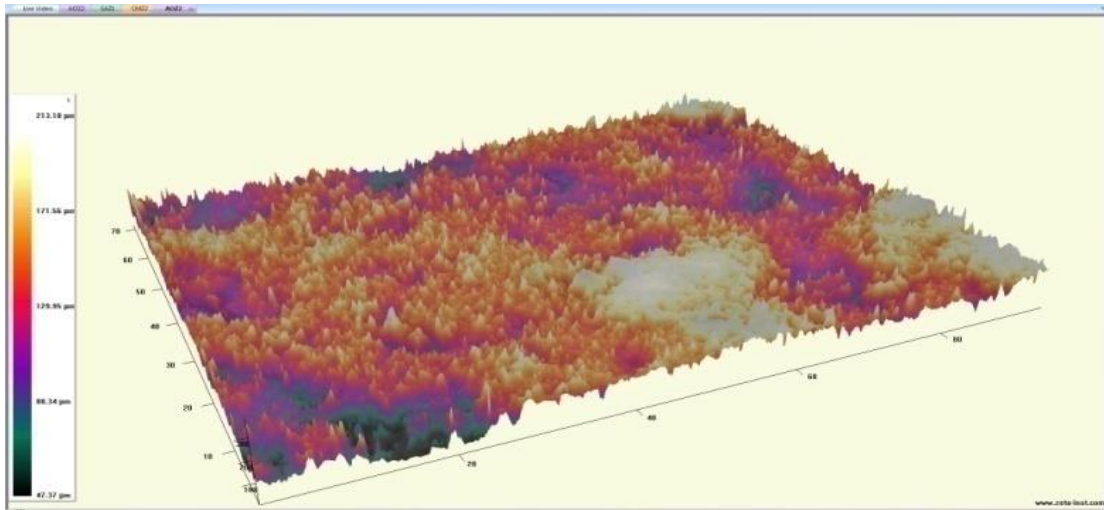


**Figure: 4.2.6 3D Optical Profilometer image of ZnO NPs**

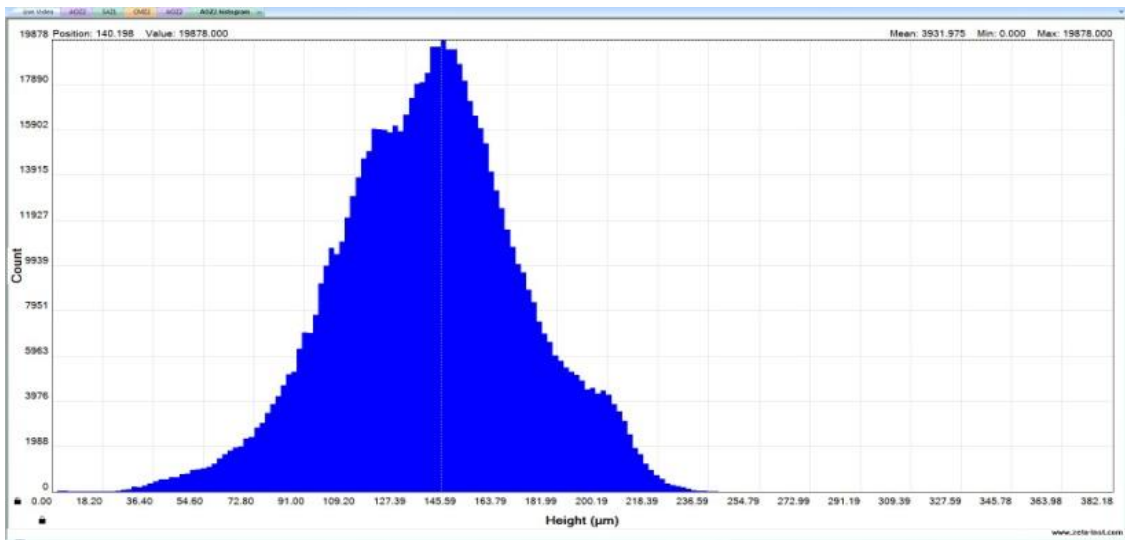
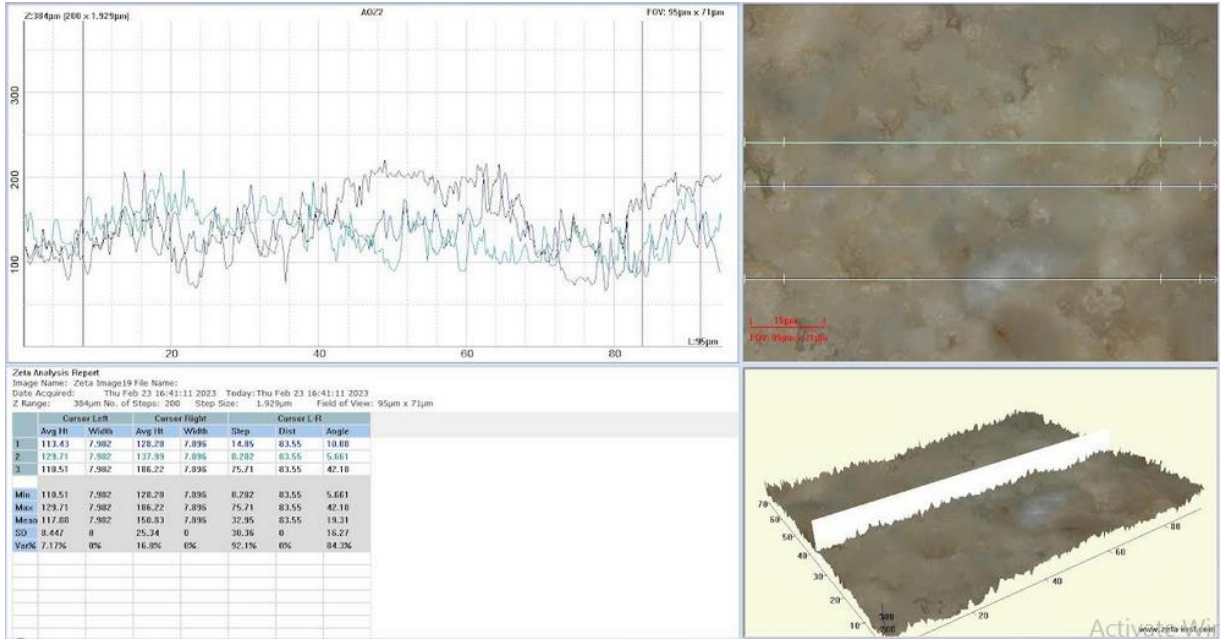


**Figure: 4.2.7 Histogram image of ZnO NPs**



Figure; 4.2.8 Cross image of ZnO-NPs

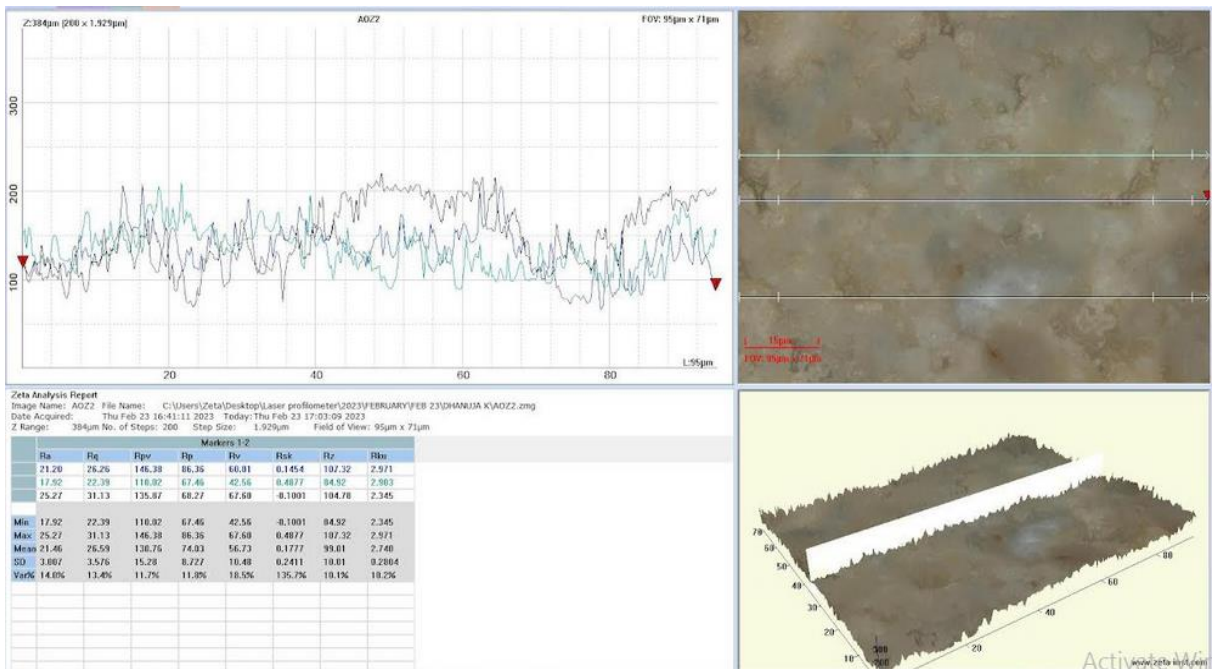


Figure: 4.2.9 Roughness image of ZnO-NPs

The surface roughness and thickness of the nanoparticles at the micrometer level are shown in Fig 4.2.8 and Fig 4.2.9 with a focus on the comparison between ZnO NPs. The roughness and thickness of nanoparticles using 3D Optical Profilometer was found to be 25.27 and 31.13 for ZnO and 110.51 and 7.982 for ZnO. ZnO NPs show a higher roughness and thickness compared to ZnO NPs. The obtained result can be explained by the fact that by blending of plant extract in the mixture solution of ZnO NPs. Crystalline size and hexagonal wurtzite structure of the ZnO NPs ensures the high purity of the nanoparticles and hence, lower crystalline size of the nanoparticles is observed to be improves the roughness and thickness of the surface

### THERMOGRAVIMERTIC ANALYSIS

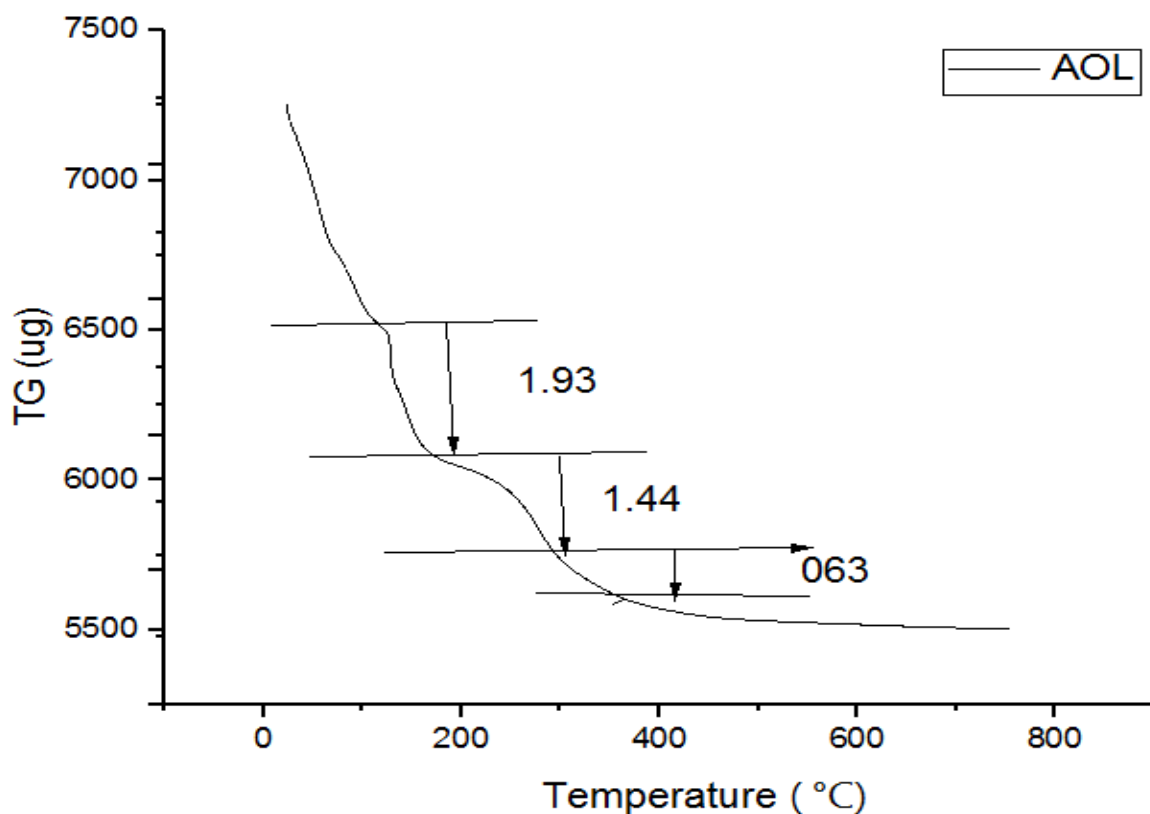
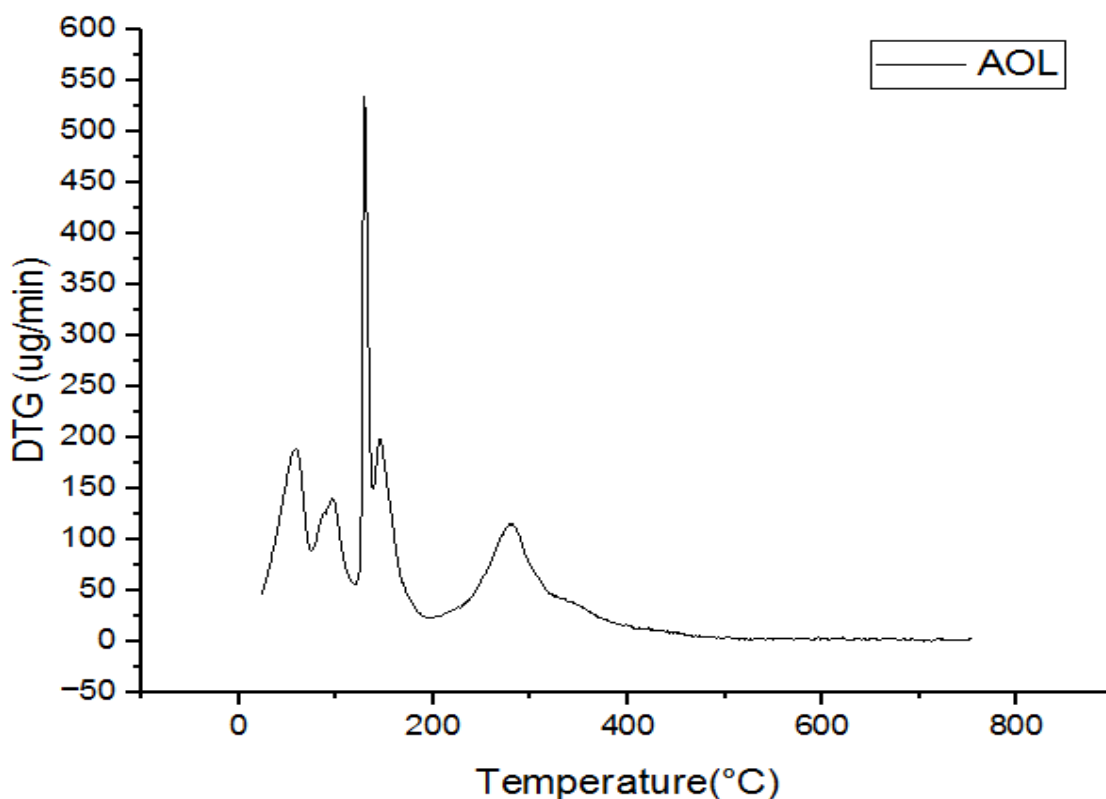


Figure: 4.2.10 TG image of ZnO NPs



**Figure; 4.2.11 TG DTG image of ZnO NPs**

Thermogravimetric analysis was conducted for the determination of thermal stability of green synthesized ZnO NPs. TGA/DTG analysis of ZnO NPs was completed at a temperature of 0 to 800°C and a rate of 10 °C/ min under an O<sub>2</sub> atmosphere and the obtained diagram is exhibited. According to the DTG curve, the weight loss of the sample was initiated in an endothermic process and reached an overall percentage of about 80%. In addition, the TGA diagram displayed three stages in which the weight loss occurred, while being completely consistent with the DTG curve. The initial step of weight loss up to 200 °C is due to water loss. i.e., the loss of physically and chemically adsorbed water molecules to the ZnO NPs. (Zoya Javed *et.al.*,2021) As the losses increase, the surface hydrophobic of ZnO NPs also enhances and results in the loss of water molecules. The second stage occurred at a range of 200 to 400 and was mainly allocated to the decomposition of

nitrate the third step was detected in the range of 350 to 800°C signified the generation of the final product in the form of ZnO-NPs. (Mahmood kermaniet.al.,2022)

### Anti-microbial activity

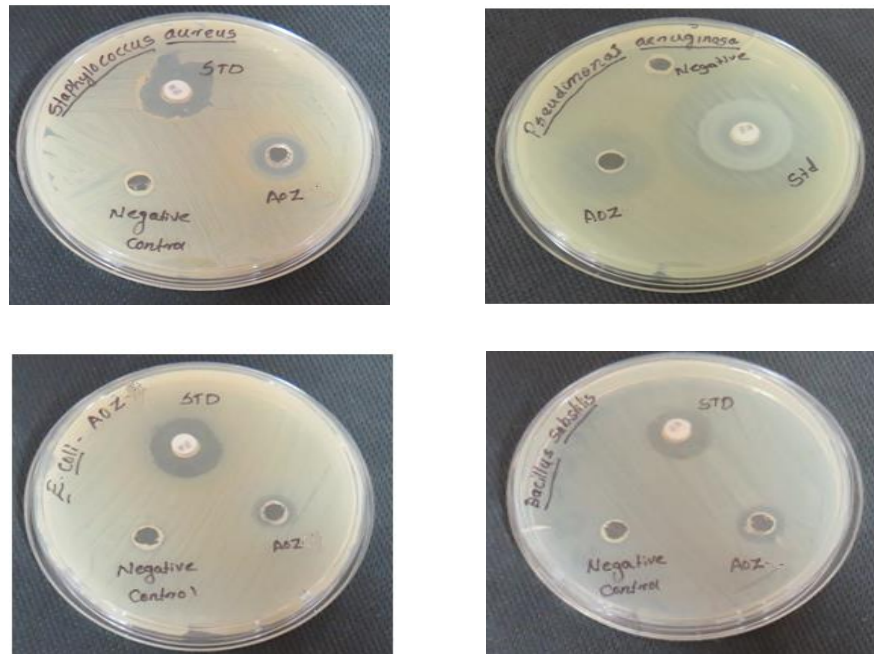


Figure: 4.2.12 Inhibition zone of ZnO NPs

Samples	Zone of Inhibition (mm)			
	<i>S.aureus</i>	<i>B.substilis</i>	<i>E.coli</i>	<i>P.aeruginos a</i>
Standard (Teicoplanin )	19	17	18	25
Negative control	0	0	0	0
<b>AOL</b>	14	11	12	21

**Table: 4.2.3 Zone of inhibition**

*Alocasia odora* leaf showed moderate antibacterial growth. *Alocasia odora* has slightly higher antibacterial activity against gram negative bacteria (*Pseudomonas aeuiginosoi*) and slightly little activity against gram positive bacterial (*Staphylous aureus* and *bacillus substills*) when compared to the teicoplanin (standard drug). (Bassant Naiel *et.al.*,2022)

### X-Ray Diffraction

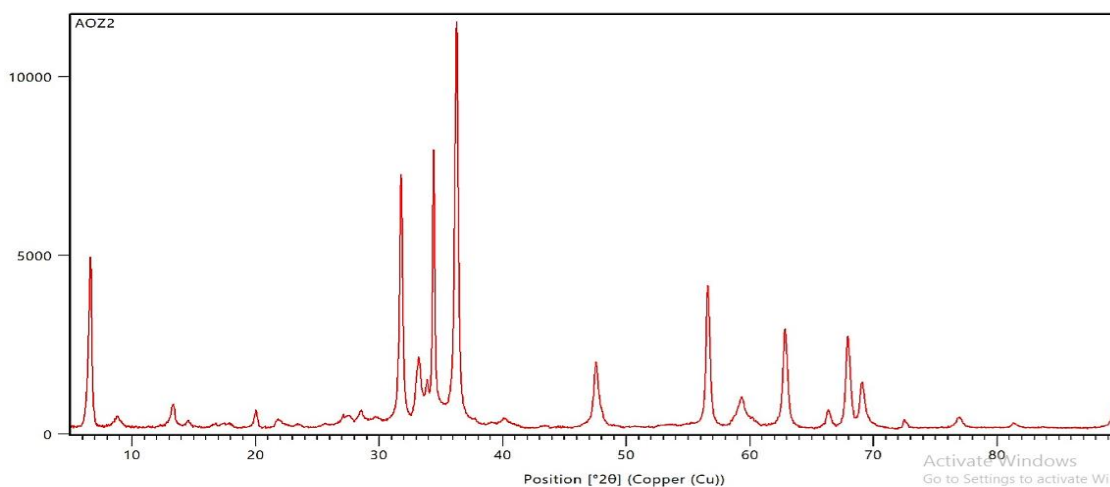


**Figure: 4.2.13 XRD image of ZnO-NPs**

XRD studies revealed the confirmation of zinc oxide nanoparticles derived from *Alocasia odora* and are given in Fig 4.2.12 The XRD pattern of ZnO nanoparticles using *Alocasia odora* extract shows peak at 25.79°, 26.35°, 33.70°, 24.50°, 17°, 23.94°, 21.54°, 22.28° corresponding to crystal planes such as 100, 002, 101, 102, 202. (Awwad et al.,2014). The XRD data of synthesized nanoparticles were matched with JPCDS NO. 89–1397 and the intensity patterns represent the hexagonal wuzurite structure. Scherrer equations were used to measure the average crystallite size.  $D = K\lambda / (\beta \cdot \cos\theta)$  where D is the average crystallite size in Å,  $\lambda$  is the wavelength of X-ray (1.5406 Å) Cu  $\alpha$  radiation, K is the shape factor (0.9)  $\beta$  is the full width half wave maximum (FWHM) of the biosynthesized nanoparticles and  $\theta$  is the diffraction angle. The crystallite size of *Alocasia odora* assisted zinc oxide nanoparticles mediated zinc oxide nanoparticles were found to be 24.39 nm. (Sadhan Kumar Chaudhuri et.al.,2017)

S.NO	Degree( 2 $\theta$ )	FWH M( $^{\circ}$ )	Crystal lite size (D)
1	6.62	0.32	25.79
2	31.77	0.36	26.35
3	34.42	0.25	33.70
4	36.25	0.35	24.50
5	47.57	0.52	17
6	56.60	0.39	23.94
7	62.95	0.45	21.57
8	67.95	0.44	22.28
Average crystallite size = <b>24.39 nm</b>			

**Table: 4.2.4 Structure and geometric parameters of green synthesis of ZnO NPs**

# *Summary and Conclusion*

## SUMMARY AND CONCLUSION

This is the first study on the photosynthesis of ZnO NPs from *Alocasia odora* leaf extract, which was utilised as a reducing agent. The production of plant extract in zinc oxide nanoparticles was validated by characterizing the synthesized nanoparticles. By using FTIR Spectroscopy, XRD, 3D Optical Profilometry, and the well diffusion method, the structural, morphological, and antibacterial activities of produced nanoparticles were characterized. According to the study's findings, *Alocasia odora* plants contains a number of naturally occurring bioactive substances that can be used to make nanoparticles. For zinc oxide, an XRD pattern revealed a structure with a crystal size of 124.39 nm. The nanoparticles were characterized by XRD, FT-IR, SEM, EDX, UV, TGA, 3D Optical Profilometer, and Antibacterial. Studies an important role in the synthesis of zinc oxide nanoparticles may have been played by biomolecules found in the plant extract, according to the results of the FT-IR investigation. SEM pictures made it abundantly evident that the synthesized *Alocasia odora* zinc oxide nanoparticles may be utilized in the sectors of water remediation and photocatalytic characteristics.

# ***Bibliography***

## Bibliography

- Chanu, T. T., & Upadhyaya, H. (2019). Zinc oxide nanoparticle-induced responses on plants: a physiological perspective. In *Nanomaterials in plants, algae and microorganisms* (pp. 43-64). Academic Press.
- Abdel Latef, A. A. H., Abu Alhmad, M. F., & Abdelfattah, K. E. (2017). The possible roles of priming with ZnO nanoparticles in mitigation of salinity stress in lupine (*Lupinus termis*) plants. *Journal of plant growth regulation*, 36, 60-70.
- Alharby, H. F., Metwali, E. M., Fuller, M. P., & Aldhebiani, A. Y. (2017). Impact of application of zinc oxide nanoparticles on callus induction, plant regeneration, element content and antioxidant enzyme activity in tomato (*Solanum lycopersicum* Mill) under salt stress.
- Alharby, H. F., Metwali, E. M., Fuller, M. P., & Aldhebiani, A. Y. (2016). The alteration of mRNA expression of SOD and GPX genes, and proteins in tomato (*Lycopersicon esculentum* Mill) under stress of NaCl and/or ZnO nanoparticles. *Saudi journal of biological sciences*, 23(6), 773-781.
- Ali, K., Dwivedi, S., Azam, A., Saquib, Q., Al-Said, M. S., Alkhedhairi, A. A., & Musarrat, J. (2016). Aloe vera extract functionalized zinc oxide nanoparticles as nanoantibiotics against multi-drug resistant clinical bacterial isolates. *Journal of colloid and interface science*, 472, 145-156.
- Ambika, Subramanian, and Mahalingam Sundrarajan. "Antibacterial behaviour of Vitex negundo extract assisted ZnO nanoparticles against pathogenic bacteria." *Journal of Photochemistry and photobiology B: Biology* 146 (2015): 52-57.
- Anbuvaran, M., Ramesh, M., Viruthagiri, G., Shanmugam, N., & Kannadasan, N. (2015). Synthesis, characterization and photocatalytic activity of ZnO nanoparticles prepared by biological method. *Spectrochimica Acta Part A: Molecular and Biomolecular Spectroscopy*, 143, 304-308.

- Chanu, T. T., & Upadhyaya, H. (2019). Zinc oxide nanoparticle-induced responses on plants: a physiological perspective. In *Nanomaterials in plants, algae and microorganisms* (pp. 43-64). Academic Press
- Bacaksiz, E. M. İ. N., Parlak, M., Tomakin, M. U. R. A. T., Özçelik, A., Karakız, M., & Altunbaş, M. (2008). The effects of zinc nitrate, zinc acetate and zinc chloride precursors on investigation of structural and optical properties of ZnO thin films. *Journal of Alloys and Compounds*, 466(1-2), 447-450.
- Banumathi, B., Malaikozhundan, B., & Vaseeharan, B. (2016). Invitro acaricidal activity of ethnoveterinary plants and green synthesis of zinc oxide nanoparticles against *Rhipicephalus (Boophilus) microplus*. *Veterinary parasitology*, 216, 93-100.
- Bhattacharyya, S., & Gedanken, A. (2008). A template-free, sonochemical route to porous ZnO nano-disks. *Microporous and Mesoporous Materials*, 110(2-3), 553-559.
- Parthasarathy, G., Saroja, M., Venkatachalam, M., Evanjelene, V. K., & Mahalakshmi, S. (2016). Bio-fabrication of zinc oxide nanoparticles using leaf extract of *Anisochilus carnosus*, and to study their characterization and antibacterial activities.
- Hussein, M. Z., Azmin, W. H. W. N., Mustafa, M., & Yahaya, A. H. (2009). *Bacillus cereus* as a biotemplating agent for the synthesis of zinc oxide with raspberry-and plate-like structures. *Journal of inorganic biochemistry*, 103(8), 1145-1150.
- Rao, G. D., Kaushik, M. P., & Halve, A. K. (2012). Zinc oxide nanoparticles: An environmentally benign and reusable catalyst for the synthesis of 1, 8-dioxo-octahydroxanthene derivatives under solvent-free conditions. *Heterocyclic Letters*, 2, 411-418.
- Jayakar, V., Lokapur, V., Nityasree, B. R., Chalannavar, R. K., Lasrado, L. D., & Shantaram, M. (2021). Optimization and green synthesis of zinc oxide nanoparticle using *Garcinia cambogia* leaf and evaluation of their antioxidant and anticancer property in kidney cancer (A498) cell lines. *Biomedicine*, 41(2), 206-222.

- P Singh, R., K Shukla, V., S Yadav, R., K Sharma, P., K Singh, P., & C Pandey, A. (2011). Biological approach of zinc oxide nanoparticles formation and its characterization. *Advanced Materials Letters*, 2(4), 313-317.
- Zhang, D., Ma, X. L., Gu, Y., Huang, H., & Zhang, G. W. (2020). Green synthesis of metallic nanoparticles and their potential applications to treat cancer. *Frontiers in Chemistry*, 8, 799.
- Redel, E., Mirtchev, P., Huai, C., Petrov, S., & Ozin, G. A. (2011). Nanoparticle films and photonic crystal multilayers from colloiddally stable, size-controllable zinc and iron oxide nanoparticles. *ACS nano*, 5(4), 2861-2869.
- Krishnakumar, V., Kumar, K. M., Mandal, B. K., & Khan, F. R. N. (2012). Flower-shaped ZnO nanoparticles as an efficient, heterogeneous and reusable catalyst in the synthesis of N-arylhomophthalimides and benzannelated isoquinolinones. *Research on Chemical Intermediates*, 38, 1881-1892.
- Yang, L. Y., Feng, G. P., & Wang, T. X. (2010). Green synthesis of ZnO<sub>2</sub> nanoparticles from hydrozincite and hydrogen peroxide at room temperature. *Materials Letters*, 64(14), 1647-1649.
- Zhang, F. (2012). Nanoparticulate Functional Materials: Green Synthesis and Application for the Degradation of Phenolic Compounds. In *Advanced Materials Research* (Vol. 476, pp. 1608-1611). Trans Tech Publications Ltd.
- Bagabas, A., Alshammari, A., Aboud, M. F., & Kosslick, H. (2013). Room-temperature synthesis of zinc oxide nanoparticles in different media and their application in cyanide photodegradation. *Nanoscale research letters*, 8, 1-10.
- Dulta, K., Koşarsoy Ağçeli, G., Chauhan, P., Jasrotia, R., & Chauhan, P. K. (2021). Ecofriendly synthesis of zinc oxide nanoparticles by *Carica papaya* leaf extract and their applications. *Journal of Cluster Science*, 1-15.
- Ansari, S. A., Husain, Q., Qayyum, S., & Azam, A. (2011). Designing and surface modification of zinc oxide nanoparticles for biomedical applications. *Food and Chemical Toxicology*, 49(9), 2107-2115.
- Chandrappa, K. G., & Venkatesha, T. V. (2012). Electrochemical synthesis and photocatalytic property of zinc oxide nanoparticles. *Nano-Micro Letters*, 4, 14-24.
- Zak, A. Khorsand, et al. "Synthesis and characterization of a narrow size

distribution of zinc oxide nanoparticles." *International journal of nanomedicine* (2011): 1399-1403

- Asokan, A., Ramachandran, T., Ramaswamy, R., Koushik, C. V., & Muthusamy, M. (2010). Preparation and characterization of zinc oxide nanoparticles and a study of the anti-microbial property of cotton fabric treated with the particles. *Journal of Textile and Apparel, Technology and Management*, 6(4).
- Espitia, P. J. P., Soares, N. D. F. F., Coimbra, J. S. D. R., de Andrade, N. J., Cruz, R. S., & Medeiros, E. A. A. (2012). Zinc oxide nanoparticles: synthesis, antimicrobial activity and food packaging applications. *Food and bioprocess technology*, 5, 1447-1464
- Parthasarathi, V., & Thilagavathi, G. (2011). Synthesis and characterization of zinc oxide nanopartilce and its application on fabrics for microbe resistant defence clothing. *International Journal of Pharmacy and Pharmaceutical Sciences*, 3(4), 392-398.
- AbdElhady, M. M. (2012). Preparation and characterization of chitosan/zinc oxide nanoparticles for imparting antimicrobial and UV protection to cotton fabric. *International journal of carbohydrate chemistry*, 2012.
- Husain, Q., Ansari, S. A., Alam, F., & Azam, A. (2011). Immobilization of *Aspergillus oryzae*  $\beta$  galactosidase on zinc oxide nanoparticles via simple adsorption mechanism. *International Journal of Biological Macromolecules*, 49(1), 37-43.
- John, S., Marpu, S., Li, J., Omary, M., Hu, Z., Fujita, Y., & Neogi, A. (2010). Hybrid zinc oxide nanoparticles for biophotonics. *Journal of Nanoscience and Nanotechnology*, 10(3), 1707-1712.
- Marczak, R., Werner, F., Gnichwitz, J. F., Hirsch, A., Guldi, D. M., & Peukert, W. (2009). Communication via electron and energy transfer between zinc oxide nanoparticles and organic adsorbates. *The Journal of Physical Chemistry C*, 113(11), 4669-4678.
- Kumar, S. A., Cheng, H. W., Chen, S. M., & Wang, S. F. (2010). Preparation and characterization of copper nanoparticles/zinc oxide composite modified electrode

and its application to glucose sensing. *Materials science and engineering: C*, 30(1), 86-91.

- Nawaz, H. R., Solangi, B. A., Zehra, B., & Nadeem, U. (2011). Preparation of nano zinc oxide and its application in leather as a retanning and antibacterial agent. *Canadian Journal on Scientific and Industrial Research*, 2(4), 164-170..
- Sricharussin, W., Threepopnatkul, P., & Neamjan, N. (2011). Effect of various shapes of zinc oxide nanoparticles on cotton fabric for UV-blocking and antibacterial properties. *Fibers and Polymers*, 12, 1037-1041
- Yumak, T., Kuralay, F., Muti, M., Sinag, A., Erdem, A., & Abaci, S. (2011). Preparation and characterization of zinc oxide nanoparticles and their sensor applications for electrochemical monitoring of nucleic acid hybridization. *Colloids and Surfaces B: Biointerfaces*, 86(2), 397-403.
- Hallaj, R., Salimi, A., Akhtari, K., Soltanian, S., & Mamkhezri, H. (2009). Electrodeposition of guanine oxidation product onto zinc oxide nanoparticles: Application to nanomolar detection of l-cysteine. *Sensors and Actuators B: Chemical*, 135(2), 632-641.
- Goharshadi, E. K., Abareshi, M., Mehrkhah, R., Samiee, S., Moosavi, M., Youssefi, A., & Nancarrow, P. (2011). Preparation, structural characterization, semiconductor and photoluminescent properties of zinc oxide nanoparticles in a phosphonium-based ionic liquid. *Materials science in semiconductor processing*, 14(1), 69-72.
- Banerjee, P., Chakrabarti, S., Maitra, S., & Dutta, B. K. (2012). Zinc oxide nanoparticles—sonochemical synthesis, characterization and application for photo-remediation of heavy metal. *Ultrasonics sonochemistry*, 19(1), 85-93.
- Hattori, Y., Mukasa, S., Toyota, H., Inoue, T., & Nomura, S. (2011). Synthesis of zinc and zinc oxide nanoparticles from zinc electrode using plasma in liquid. *Materials Letters*, 65(2), 188-190.
- Hattori, Y., Mukasa, S., Toyota, H., Inoue, T., & Nomura, S. (2011). Synthesis of zinc and zinc oxide nanoparticles from zinc electrode using plasma in liquid. *Materials Letters*, 65(2), 188-190.

- Tayel, A. A., EL-TRAS, W. F., Moussa, S., EL-BAZ, A. F., Mahrous, H. O. D. A., Salem, M. F., & Brimer, L. E. O. N. (2011). Antibacterial action of zinc oxide nanoparticles against foodborne pathogens. *Journal of Food Safety*, 31(2), 211-218.
- Kansal, S. K., Ali, A. H., Kapoor, S., & Bahnemann, D. W. (2011). Synthesis of flower like zinc oxide nanostructure and its application as a photocatalyst. *Separation and purification technology*, 80(1), 125-130.
- Liu, Y., Zong, S., & Li, J. (2020). Attenuation effects of bulk and nanosized zno on glucose, lipid level, and inflammation profile in obese mice. *Applied biochemistry and biotechnology*, 190, 475-486.
- Chawla, S., & Pundir, C. S. (2012). An amperometric hemoglobin A1c biosensor based on immobilization of fructosyl amino acid oxidase onto zinc oxide nanoparticles–polypyrrole film. *Analytical biochemistry*, 430(2), 156-162.
- Rekha, K., et al. "Structural, optical, photocatalytic and antibacterial activity of zinc oxide and manganese doped zinc oxide nanoparticles." *Physica B: Condensed Matter* 405.15 (2010): 3180-3185.
- Kumari, Latha, et al. "Zinc oxide micro-and nanoparticles: synthesis, structure and optical properties." *Materials Research Bulletin* 45.2 (2010): 190-196.
- B Djurisić, A., X. Y Chen, and Y. H Leung. "Recent progress in hydrothermal synthesis of zinc oxide nanomaterials." *Recent patents on nanotechnology* 6.2 (2012): 124-134.
- Przybyszewska, M., and M. Zaborski. "The effect of zinc oxide nanoparticle morphology on activity in crosslinking of carboxylated nitrile elastomer." *Express Polym. Lett* 3.9 (2009): 542-552.
- Aydin Sevinç, Berdan, and Luke Hanley. "Antibacterial activity of dental composites containing zinc oxide nanoparticles." *Journal of Biomedical Materials Research Part B: Applied Biomaterials* 94.1 (2010): 22-31.
- Malhotra, Y., Roy, S., Srivastava, M. P., Kant, C. R., & Ostrikov, K. (2009). Extremely non-equilibrium synthesis of luminescent zinc oxide nanoparticles through energetic ion condensation in a dense plasma focus device. *Journal of Physics D: Applied Physics*, 42(15), 155202. Hayat, Khizar, et al. "Nano ZnO

synthesis by modified sol gel method and its application in heterogeneous photocatalytic removal of phenol from water." *Applied Catalysis A: General* 393.1-2 (2011): 122-129.

- Boonyanitipong, Prapatsorn, et al. "Effects of zinc oxide nanoparticles on roots of rice *Oryza sativa* L." *Int Conf Environ BioSci*. Vol. 21. 2011
- Fabrega, Julia, et al. "Sequestration of zinc from zinc oxide nanoparticles and life cycle effects in the sediment dweller amphipod *Corophium volutator*." *Environmental Science & Technology* 46.2 (2012): 1128-1135.
- Bajpai, S. K., Chand, N., & Chaurasia, V. (2010). Investigation of water vapor permeability and antimicrobial property of zinc oxide nanoparticles-loaded chitosan-based edible film. *Journal of Applied Polymer Science*, 115(2), 674-683
- George, S., Pokhrel, S., Xia, T., Gilbert, B., Ji, Z., Schowalter, M., ... & Nel, A. E. (2010). Use of a rapid cytotoxicity screening approach to engineer a safer zinc oxide nanoparticle through iron doping. *ACS nano*, 4(1), 15-29.
- Baek, M., Chung, H. E., Yu, J., Lee, J. A., Kim, T. H., Oh, J. M. & Choi, S. J. (2012). Pharmacokinetics, tissue distribution, and excretion of zinc oxide nanoparticles. *International journal of nanomedicine*, 3081-3097.
- Chatterjee, T., Chakraborti, S., Joshi, P., Singh, S. P., Gupta, V., & Chakrabarti, P. (2010). The effect of zinc oxide nanoparticles on the structure of the periplasmic domain of the *Vibrio cholerae* ToxR protein. *The FEBS journal*, 277(20), 4184-4194.
- Ghosh, A., Sharma, R., Ghule, A., Taur, V. S., Joshi, R. A., Desale, D. J., ... & Han, S. H. (2010). Low temperature LPG sensing properties of wet chemically grown zinc oxide nanoparticle thin film. *Sensors and Actuators B: Chemical*, 146(1), 69-74
- Puetz, A., Stubhan, T., Reinhard, M., Loesch, O., Hammarberg, E., Wolf, S., ... & Lemmer, U. (2011). Organic solar cells incorporating buffer layers from indium doped zinc oxide nanoparticles. *Solar energy materials and solar cells*, 95(2), 579-585.

- Elilarassi, R., & Chandrasekaran, G. (2010). Synthesis and optical properties of Ni-doped zinc oxide nanoparticles for optoelectronic applications. *Optoelectronics letters*, 6(1), 6-10.
- Tayel, A. A., EL-TRAS, W. F., Moussa, S., EL-BAZ, A. F., Mahrous, H. O. D. A., Salem, M. F., & Brimer, L. E. O. N. (2011). Antibacterial action of zinc oxide nanoparticles against foodborne pathogens. *Journal of Food Safety*, 31(2), 211-218.